The enigma of relict large sorted stone stripes in the tropical Ethiopian Highlands

Alexander R. Groos[1], Janik Niederhauser[1], Luise Wraase[2], Falk Hänsel[2], Thomas Nauss[2], Naki Akçar[3], and Heinz Veit[1]

[1]Institute of Geography, University of Bern, 3012 Bern, Switzerland
[2]Department of Geography, Philipps University of Marburg, 35032 Marburg, Germany
[3]Institute of Geological Sciences, University of Bern, 3012 Bern, Switzerland

Correspondence: Alexander R. Groos (alexander.groos@giub.unibe.ch)

Abstract. Large sorted patterned grounds are one of the most prominent features of periglacial and permafrost environments of the mid-latitudes and polar regions, but were unknwon for the tropics. Here, we report on relict large sorted stone stripes (up to 1000 m long, 15 m wide, and 2 m deep) on the ca. 4000 m high central Sanetti Plateau of the tropical Bale Mountains in the southern Ethiopian Highlands. These geomorphic features are enigmatic since patterned grounds exceeding several metres are commonly associated with distinct seasonal ground temperatures, oscillating around 0 °C. For a systematic investigation of present frost phenomena and relict periglacial landforms in the Bale Mountains, we conducted extensive geomorphological mapping. The sorted stone stripes were studied in more detail by applying aerial photogrammetry, ground-penetrating radar measurements, and ^{36}Cl surface exposure dating. In addition, we installed ground temperature data logger between 3877 and 4377 m to analyse present frost occurrence and seasonal ground temperature variations. Superficial nocturnal ground frost was measured at 35-90 days per year, but the ground beneath the upper few centimetres remains unfrozen the entire year. Seasonal frost occurrence would require a mean annual ground temperature depression of about 11 °C, corresponding to an air temperature decrease of about 6-8 °C (relative to today) as inferred from a simple statistical ground temperature model experiment. Our results suggest a formation of the large sorted stone stripes under past periglacial conditions related to lateral and vertical frost sorting in the course of cyclic freezing and thawing of the ground. It is likely that the stone stripes formed either in proximity of a former ice cap on the Sanetti Plateau due to seasonal frost heave and sorting over the last glacial period or they developed over multiple cold phases during the Pleistocene. Although certain aspects of the genesis of the large sorted stone stripes remain unresolved, the presence of these geomorphic features provides independent evidence besides glacial landforms for unprecedented palaeoclimatic and palaeoenvironmental changes in the tropical Bale Mountains during the (Late) Pleistocene.

1 Introduction

Sorted patterned grounds in the form of stone polygons, circles or stripes are one of the most striking features of periglacial and permafrost environments. They are known from the Arctic (e.g. Nicholson, 1976; Hallet, 2013), Antarctic (e.g. Hallet et al., 2011), mid-latitudes (e.g. Richmond, 1949; Miller et al., 1954; Ball and Goodier, 1968; André et al., 2008), and high

mountains (e.g. Francou et al., 2001; Matsuoka, 2005; Bertran et al., 2010), and were even detected on other celestial bodies like Mars (e.g. Mangold, 2005; Balme et al., 2009). Sorted stone polygons are found in flat areas while stripes typically occur on slightly inclined slopes. Both forms are the product of a self-organising process related to the cyclic freezing and thawing of the ground (Kessler and Werner, 2003). Small-scale patterned grounds in the order of centimetres to decimetres are common on many mid-latitude and high tropical mountains as superficial nocturnal frost is sufficient for their formation (e.g. Francou et al., 2001; Matsuoka, 2005). On the contrary, large sorted forms (with several metres in diameter) occur almost exclusively in permafrost areas where the mean annual air temperature is far below 0 °C (Goldthwait, 1976). Active large sorted stone circles, polygons, and stripes are well-documented for the High Arctic (e.g. Washburn, 1980; Kessler and Werner, 2003; Hallet, 2013) and in relict form also for some mid-latitude mountains (e.g. Ball and Goodier, 1968; Vopata et al., 2006; André et al., 2008; Křížek et al., 2019), but they have not yet been reported for any site in the tropics.

The absence of large sorted patterned grounds in the tropics could generally be explained by the warm tropical climate, the intense solar radiation, and minor seasonal temperature fluctuations. However, the missing observation of such landforms could also be partly due to the remoteness of many mountains and the resulting lack of geomorphological investigations. An enigmatic relict landform similar to the large sorted stone stripes known from the mid-latitudes and polar regions has been reported from the ca. 4000 m high central Sanetti Plateau of the tropical Bale Mountains in the southern Ethiopian Highlands (Miehe and Miehe, 1994). The stone stripes on the southern part of the Sanetti Plateau are several metres wide and tens of metres long. They are located on the slope of an eroded volcanic plug and have therefore originally been termed "trenched boulder slopes" (Miehe and Miehe, 1994; Osmaston et al., 2005). Grab (2002) pointed out that the large – and for the tropics unique – dimension of the stone stripes may be an indicator for past sporadic permafrost on the plateau. However, a systematic investigation of the relict as well as present geomorphological processes and landforms on the Sanetti Plateau has not yet been performed. When and how the stone stripes formed and what their occurrence implies for the palaeoclimate and palaeoenvironment of the southern Ethiopian Highlands is still unexplored.

Information regarding the age and genesis of the large sorted stone stripes are essential for the reconstruction of the palaeoenvironment of the Bale Mountains. Recent glacial geomorphological and chronological investigations revealed that the Bale Mountains were extensively glaciated during the Late Pleistocene and experienced a pronounced cooling of at least 5.2 ± 0.8 °C during the local Last Glacial Maximum between 28-42 ka (Groos et al., in revision). Since the stone stripes are located near the former margin of the ice cap on the Sanetti Plateau, it can be hypothesised that the stone stripes evolved under periglacial conditions during the last glacial period. If cyclic freezing and thawing of the ground was indeed one of the preconditions for the formation of the stone stripes on the plateau, they could serve as potential climate proxy. The deviation of the present mean annual ground temperature (MAGT) from the freezing point (0 °C) would then provide a minimum estimate for the ground temperature depression (relative to today) during the period when the stone stripes formed.

The aim of this study is a first systematic investigation of the relict large sorted stone stripes and contemporary frost dynamics and phenomena on the Sanetti Plateau. To analyse the distribution of relict and active periglacial landforms, we conducted extensive geomorphological mapping in the field supported by the analysis of high-resolution satellite images. The geometry and internal structure of the sorted stone stripes was studied in more detail based on Unmanned Aerial Vehicle (UAV) and ground-penetrating radar (GPR) surveys. Top surfaces of six rocks from two different stone stripes were sampled for ^{36}Cl surface exposure dating. The ^{36}Cl data were published by Groos et al. (in revision) in a palaeoglaciological context, but because of their relevance for the interpretation of the genesis of the stone stripes, we present them here again. Since knowledge on present frost occurrence and ground temperature variations is indispensable for discussing how and under which climatic and environmental conditions the relict structures formed, we installed thirteen ground temperature data loggers at six different locations on the Sanetti Plateau (Fig. 1). In a final step, we combined the ground temperature measurements with meteorological data from nearby weather stations and applied a simple statistical model experiment to infer the minimum air temperature depression theoretically needed for seasonal ground frost on the plateau (MAGT ~ 0 °C).

2 Study area

The Bale Mountains (6.6–7.1 °N, 39.5–40.0 °E) are located southeast of the Main Ethiopian Rift and belong to the Bale-Arsi massif, which constitutes the western part of the southern Ethiopian Highlands (Fig. 1). Precambrian rocks and overlying Mesozoic marine sediments form the base of the massif and are covered by Cenozoic trachytic and basaltic lava flows (Miehe and Miehe, 1994; Osmaston et al., 2005; Hendrickx et al., 2014). Due to the lack of geological maps, lithological information, geochemical studies, and radiometric dating, especially in the southern Ethiopian Highlands, the exact timing of volcanic eruptions in the region is unknown and the successive formation of the Bale-Arsi massif still poorly understood (Mohr, 1983; Osmaston et al., 2005). Characteristic for the Bale Mountains is the central Sanetti Plateau with a mean elevation of about 4000 m. It is bounded to the west by extensive lava flows, to the north and east by broad U-shaped valleys, and to the south by the Harenna Escarpment. Several volcanic plugs and cinder cones like the highest peak Tullu Dimtu (4377 m) rise above the plateau (Osmaston et al., 2005). With an area of almost 2000 km² above 3000 m, the Bale Mountains comprise Africa's most extensive tropical alpine environment (Groos et al., in revision). Hedberg (1951) defined the afro-alpine belt in tropical Africa as the area above ~3500 m. Others set the lower elevation of the tropical afro-alpine belt to 3200 m (e.g. de Deus Vidal Junior and Clark). The Bale Mountains are an important fresh water source for the surrounding lowlands. The main tributaries of the only two perennial rivers in the Somali lowlands, Shebelle and Jubba, originate from the Bale Mountains.

The seasonal movement of the Intertropical Convergence Zone (ITCZ) and zonal shift of the Congo Air Boundary as divide of air masses from the Indian Ocean and Atlantic determine the climate and rainfall patterns of the Ethiopian Highlands (Levin et al., 2009; Tierney et al., 2011; Costa et al., 2014). Due to the complex topography, the mean annual precipitation varies considerably across the region and is strongly controlled by elevation (Gebrechorkos et al., 2019). Three seasons characterise the current climate: The dry season lasts from November to February and is followed by two rainy seasons. While the first rainy

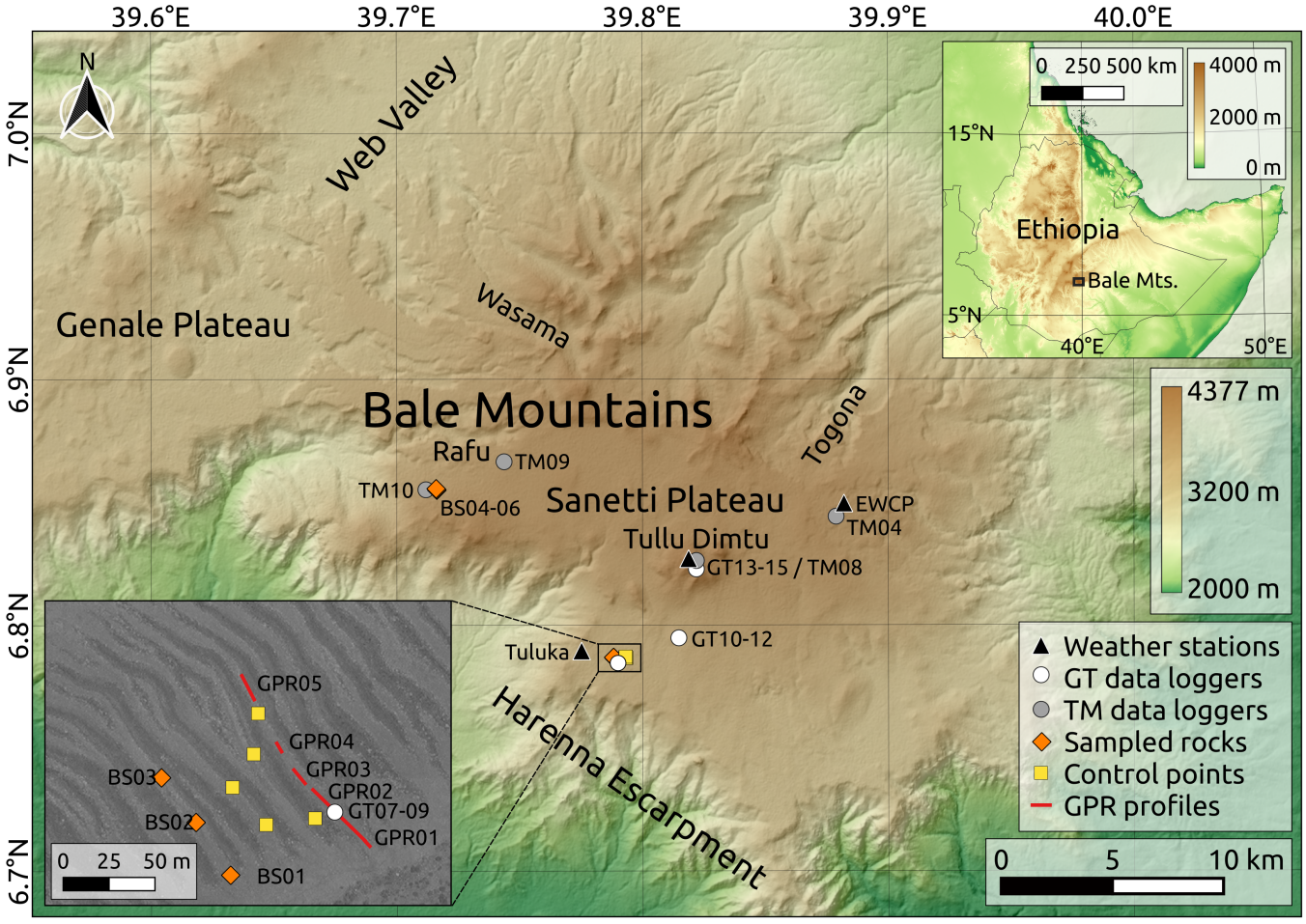

Figure 1. Overview map of the experimental setup and observational network in the Bale Mountains (southern Ethiopian Highlands), located in the Horn of Africa. The automatic weather stations as well as the high-quality (GT) and low-cost (TM) ground temperature data loggers on the Sanetti Plateau were installed in January and February 2017. Unmanned Aerial Vehicle and Ground-Penetrating Radar surveys were performed to obtain information on the morphology and internal structure of the stone stripes (see GPR profiles in the lower left map inset). Six rocks from two different stone stripes were sampled for surface exposure dating. Data basis: SRTM 1 Arc-Second Global (United States Geological Survey) for the main map and upper right inlet, high-resolution WorldView-1 satellite image (DigitalGlobe Foundation) for the lower left inlet. Ground control points (i.e. natural objects; yellow squares in the inlet) visible in both the georectified WorldView-1 image and the UAV images served for the georeferencing of the UAV data.

season (March to June) is more pronounced in the southern Ethiopian Highlands, the second one (July to October) is more important in the northern highlands including the upper catchment area of the Blue Nile (Conway, 2000; Seleshi and Zanke, 2004). Relatively dry northeasterly trade winds from the Arabian Peninsula and Sea prevail in the Bale Mountains during the dry season as a result of the large-scale atmospheric circulation (i.e. location of the ITCZ south of the equator and persistence

of high pressure cells over Western Asia and the Sahara). Along with the northward movement of the ITCZ from March to June, the main wind direction changes from northeast to southeast and brings moist air from the southern Indian Ocean to the Bale Mountains (Lemma et al., 2020). Although the Gulf of Guinea and Congo Basin are important moisture sources for the northern Ethiopian Highlands (Levin et al., 2009; Viste and Sorteberg, 2013; Costa et al., 2014), they seem of minor relevance for the Bale-Arsi massif (Lemma et al., 2020). The Sanetti Plateau and highest peaks of the massif experience occasional snowfall during the rainy seasons, but the thin snowpack usually melts within hours or days (Miehe and Miehe, 1994).

3 Data and methods

3.1 Mapping of periglacial landforms

Comprehensive geomorphological mapping of glacial and periglacial landforms provides crucial data for reconstructing the palaeoenvironment and palaeoclimate of polar and alpine regions (Chandler et al., 2018). We studied maps, photographs, and field notes from previous studies dealing with periglacial processes and landforms in the Bale Mountains (e.g. Messerli and Winiger, 1992; Miehe and Miehe, 1994; Grab, 2002; Umer et al., 2004; Osmaston et al., 2005) to compile evidence of relict and modern frost occurrence. Since periglacial landforms have not yet been described systematically, we performed extensive geomorphological mapping on the Sanetti Plateau, along the upper Harenna Escarpment, and in the western, northern, and eastern valleys during multiple field trips between 2016 and 2020 (Fig. 2a). In addition, we analysed high-resolution WorldView-1 satellite images (pixel size = 0.5 m) provided by the DigitalGlobe Foundation to identify geomorphic features in remote areas of the mountain range. All periglacial landforms and other geomorphological features mapped in the field or on satellite images were compiled in a catalogue (see Table A1).

3.2 UAV-based aerial surveys

For a detailed analysis of the geometry and clast size distribution of the stone stripes on the Sanetti Plateau, we conducted a manual aerial survey (~50 m above ground level) with a small quadcopter (DJI Mavic Pro) on the 30th January 2020 at 2 pm local time. In total, 75 aerial images were acquired during the survey and were processed with the photogrammetric software OpenDroneMap (following the general approach described in Groos et al., 2019) to obtain a high-resolution orthophoto (5 cm) and digital surface model (DSM, 10 cm) of the stone stripes. Five natural objects (rocks and dwarf shrubs) visible both in the orthorectified WorldView-1 image and at least in three aerial images were used as ground control points (Fig. 1) to process and georeference the UAV data (see Groos et al., 2019). The necessary elevation information were extracted from the SRTM 1 Arc-Second Global dataset. It was not possible to measure the ground control points directly in the field as a differential Global Positioning System was not available. In principle, a small number of ground control points is sufficient to generate an accurate DSM without any larger deformation if the surveyed area is very small (i.e. 60 x 80 m) (e.g. James and Robson, 2014; Gindraux et al., 2017). The horizontal (XY) accuracy of the final orthophoto is ~0.3 m (relative to the orthorectified WorldView-1 image) and the vertical (Z) accuracy of the DSM is ~0.8 m (relative to the SRTM-1 DEM). The absolute positional accuracy of the

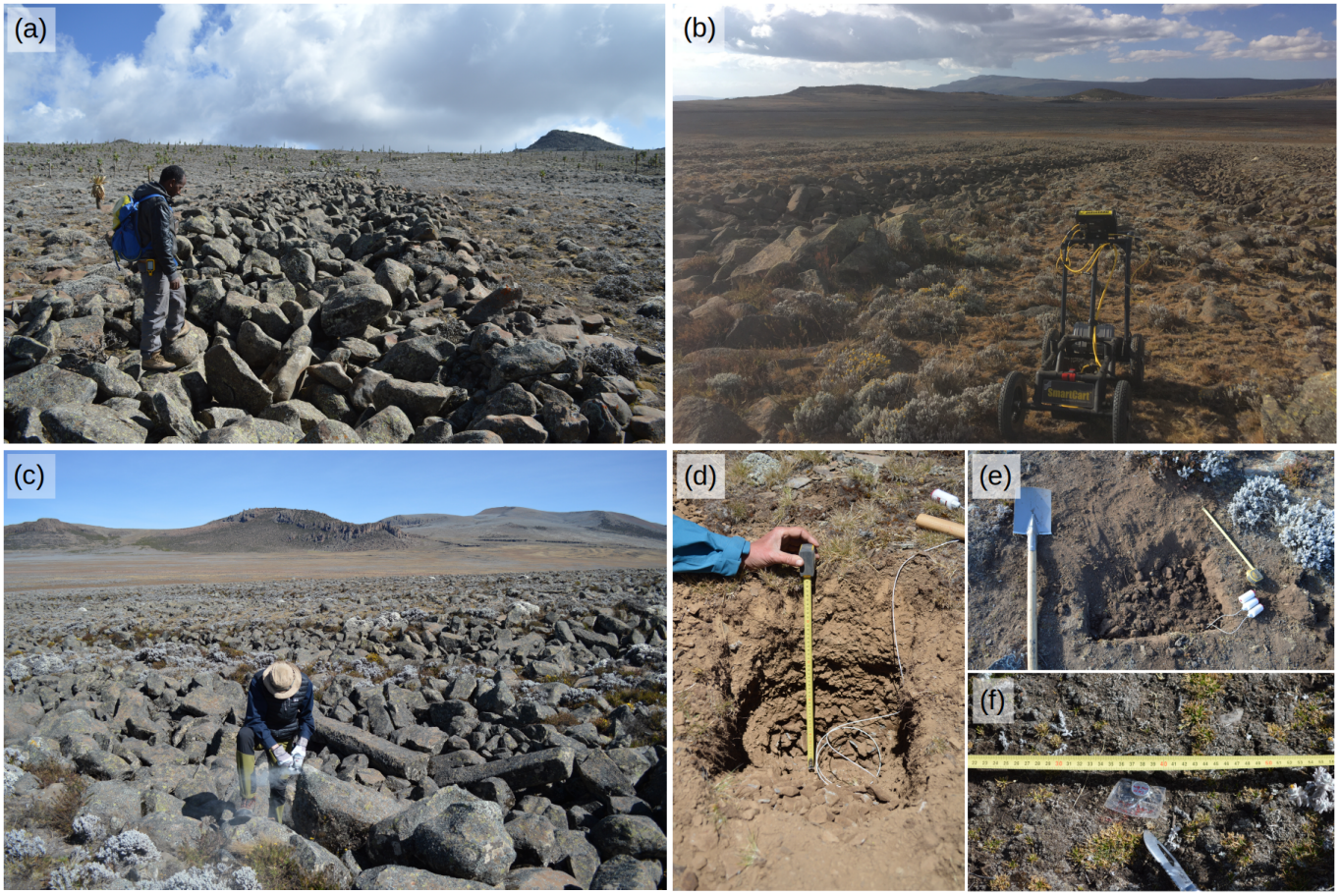

Figure 2. Field work in the Bale Mountains: (a) reconnaissance and mapping of periglacial landforms, (b) ground-penetrating radar survey, (c) sampling of stone stripes for surface exposure dating, (d-f) installation of ground temperature loggers.

orthophoto and DSM might be larger, but this can be neglected as the UAV data are not compared with other datasets. The internal accuracy of the orthophoto and DSM is in the order of just a few centimetres to decimetres.

3.3 Ground-penetrating radar measurements

Information on the internal structure of the coarse stone and fine regolith stripes (i.e. sorting depth, presence/absence of cryoturbation features, etc.) are essential to study the genesis of this landform. However, investigating the internal structure of the sorted stone stripes by excavating a transect was conflicting with the park rules. As an alterantive we performed a ground-penetrating radar (GPR) survey between two stripes on the southern Sanetti Plateau on the 10th February 2020 (Fig. 2b). We made use of a Pulse EKKO PRO GPR with a 1000 MHz antenna (7.5 cm sensor width) manufactured by Sensors & Software Inc. (for system settings see Table B1). The GPR was mounted on a compatible pushcart. As survey setting, an exploration

depth of 1 m and pulse length of 16 nanoseconds (ns) was applied for the first line and modified to 1.5 m depth and 24 ns pulse length for the following lines. The starting point of the GPR measurement was located 10 m above the position of the data loggers GT07-09. The uppermost part of the volcanic plug was not accessible with the pushcart. Due to uneven terrain and several natural obstacles like smaller stones and dwarf shrubs, the GPR profile between the two stone stripes was split into five separate lines varying between 3.8 and 38.5 m in length. The chaotic structure of the stones stripes prevented a GPR survey inside the troughs and coarse material. We used the software EKKO Project (version 5.0) for the analysis and visualisation of the GPR data.

3.4 ^{36}Cl surface exposure dating

Previous studies have shown that the stabilisation age of periglacial landforms like rock glaciers and block fields can be successfully dated with cosmogenic nuclides (e.g. Barrows et al., 2004; Ivy-Ochs et al., 2009; Steinemann et al., 2020). We sampled two sorted stone stripes on the Sanetti Plateau (Fig. 1) to exposure date the stabilisation phase of these features. From both stone stripes, we selected three boulders for ^{36}Cl surface exposure dating (Table C1). To avoid any uncertainties related to the shielding or toppling of rocks after the stabilisation phase, we chose only boulders that were sticking out and were wedged between other boulders (Fig. 2c). The upper few centimetres of each boulder were sampled with hammer, chisel, and angle grinder for the subsequent laboratory analysis. An inclinometer was used in the field for measuring the topographic shielding. For extraction of the isotope ^{36}Cl, the six samples were crushed, sieved and chemically treated in the Surface Exposure Dating Laboratory of the University of Bern. Total Cl and ^{36}Cl concentrations (Table C2) were measured from one target at the 6 MV Accelerator Mass Spectrometre (AMS) fascility at the ETH Zurich using the isotope dilution technique (Ivy-Ochs et al., 2004) and a gas-filled magnet to separate ^{36}S (Vockenhuber et al., 2019). Surface exposure ages were calculated from the measured Cl and ^{36}Cl concentrations with the latest version (2.1) of the CRONUS Earth Web Calculator (http://cronus.cosmogenicnuclides.rocks/2.1/html/cl/) using the physics-based and time-dependent Lifton-Sato-Dunai scaling framework (Lifton et al., 2014; Marrero et al., 2016). For a detailed description of the sample preparation, Cl and ^{36}Cl measurements, and surface exposure age calculation see Groos et al. (in revision).

3.5 Ground temperature measurements

For measuring hourly ground temperatures on the Sanetti Plateau, we installed high-quality UTL-3 Scientific Dataloggers (hereafter GT data loggers) in 2, 10, and 50 cm depth at two different stone stripe locations and on Tullu Dimtu, covering an elevation between 3877 and 4377 m (Fig. 1 and Table D1). The GT data loggers were developed by GEOTEST Ltd. in collaboration with the Swiss Institute for Snow and Avalanche Research. The measurement accuracy is <0.1 °C at 0 °C. At each of the three measurement sites, the upper 50 cm of the ground were removed to install the GT data loggers (Fig. 2d,e). We used data loggers with an external cable and thermistor for the measurements in 10 and 50 cm depth. A standard logger without external cable was placed just below the surface in 2 cm depth. After the installation, each hole was filled in the same order as during the excavation to ensure as little disturbance of the profile as possible. Additional low-cost tempmate.-B temperature data loggers (hereafter TM data loggers) in the size of a button cell (Fig. 2f) were distributed on the plateau between 4022 and

4377 m to increase the spatial coverage of near-surface (2 cm) hourly ground temperature measurements (Fig. 1 and Table D1). The measurement accuracy is ± 0.5 °C in the range of -10 to 65 °C.

Several issues occurred during the measurement period from January 2017 to January 2020 and caused longer data gaps. On Tullu Dimtu, data loggers GT13-15 were removed in May 2017, but could be recovered and reinstalled in January 2018. Individual outliers and longer periods with implausible measurements were deleted from the time series. Data logger GT07 was accidentally placed in 6 cm depth and not in 2 cm as intended. The relocation towards the surface after the first readout in December 2017 led to an abrupt increase in the temperature amplitude. Therefore, we calculated hourly ground temperature gradients between 6 and 10 cm depth from GT07 and GT08 data by applying a simple linear regression to extrapolate the GT07 measurements from 6 to 2 cm in the period 21st January to 10th December 2017. Data gaps in individual time series of the data loggers were filled using a simple linear regression and available data from other GT or TM loggers to generate a complete data set for the period 1st February 2017 to 20th January 2020. We analysed the interpolated hourly ground temperature data statistically to quantify frost occurrence and spatio-temporal ground temperature variations on the Sanetti Plateau.

3.6 Meteorological measurements

Within the framework of the DFG Research Unit 2358, automatic weather stations (AWS) were installed inter alia on the Sanetti Plateau between 3848 and 4377 m beginning of 2017 (Table D2). The AWS are manufactured by Campbell Scientific and consist of a three metre galvanised tubing tripod, a grounding kit, a weather-resistant enclosure, a measurement and control system (CR800), a solar module (SDT200), a 168 Wh battery, a charging regulator, a temperature and relative humidity probe (CS215) with radiation shield, a pyranometer (LI-200R), a two-dimensional ultrasonic anemometer from Gill Instruments, and a rain gauge from Texas Electronics (TR-525USW 8"). For protection, the AWS are wire-fenced by a 3 x 3 m compound. Air temperature, relative humidity, and global radiation are measured at 2 m height, wind speed and wind direction at 2.6 m height, and precipitation at 1 m height. The measurement interval is 15 minutes. All measured variables are finally aggregated to hourly averages. The AWS installed in the southern and northern part of the Sanetti Plateau measured quasi continously, but the time series of the AWS on the central peak Tullu Dimtu was interrupted due to issues with the power supply (Table D2). The hourly meteorological data from the different AWS are stored in an online database and gaps in the time series of all variables except wind speed and direction are interpolated statistically as described by Wöllauer et al. (2020).

3.7 Ground temperature modelling experiment

The potential of periglacial landforms for paleoclimatic and environmental reconstructions has already been pointed out in pioneering studies from more than half a century ago (e.g. Galloway, 1965). For polar and alpine regions, where stone circles and other patterned grounds form, ground temperatures oscillate typically around 0 °C (e.g. Hallet, 2013). If cyclic freezing and thawing of the ground was one of the drivers for the formation of the stone stripes on the Sanetti Plateau, this landform may serve as a potential climate proxy. The deviation of the present mean annual ground temperature (MAGT) from the freezing point (0 °C) would provide a minimum estimate for the ground temperature depression (relative to today) during the period

when the stone stripes formed. Here, we apply a simple statistical modelling experiment to infer which climatic conditions would theoretically promote a MAGT of ca. 0 °C on the Sanetti Plateau. We first established a statistical correlation between ground temperature and a set of meteorological variables. For the development of separate multiple linear regression models, we considered three locations on the Sanetti Plateau where ground temperatures and meteorological variables were measured simultaneously (Tullu Dimtu, EWCP Station, Tuluka). We chose only air temperature and global radiation as explanatory variables. The wind speed time series contains data gaps, precipitation is limited to individual rain events, and relative humidity does not show a direct linear relationship with ground temperature (see Fig. E1). The multiple linear regression model at each site was calibrated for the period 1st February 2017 – 31st January 2019 and validated for the period 1st February 2019 – 20th January 2020. Present-day hourly ground temperatures in 2 cm (T_{2cm}) can then be modelled using measured air temperature and incoming shortwave radiation:

$$T_{\mathrm{2cm,i}} = \beta_0 + (\beta_1 \times T_{\mathrm{air,i}}) + (\beta_2 \times Q_{\mathrm{S,i}}), \quad (1)$$

where $T_{air,i}$ ($i = 1,\ldots,n$) is the hourly measured air temperature in °C, $Q_{S,i}$ is the hourly measured incoming shortwave radiation in W m^{-2}, β_0 is the intercept, β_1 is the coefficient for T_{air}, and β_2 is the coefficient for Q_S. The coefficients and goodness of fit for each of the three linear models are provided in Table E1. For simulating a decrease in ground temperature, two additional parameters, ΔT_{air} and ΔQ_S, were introduced:

$$T_{\mathrm{2cm,i}} = \beta_0 + (\beta_1 \times (T_{\mathrm{air,i}} - \Delta T_{\mathrm{air}})) + (\beta_2 \times (Q_{\mathrm{S,i}} - \Delta Q_{\mathrm{S}})), \quad (2)$$

where ΔT_{air} is the air temperature depression of interst (in °C) and ΔQ_S is the difference between the mean present-day and past incoming shortwave radiation in W m^{-2}. For simplicity, we set ΔQ_S to 30 W m^{-2} (the rough lowering of incoming shortwave radiation during MIS 2 at 15 °N, see Groos et al., in revision). To infer the air temperature depression of interest using *Eq.* 2, we increased ΔT_{air} (starting with: ΔT_{air} = 0 °C) with every iteration until the MAGT ($\overline{T}_{2cm}$) became smaller 0°C. We tested all three developed multiple linear regression models (Tullu Dimtu, EWCP Station, and Tuluka) to quantify the uncertainty of the approach originating from differences in the model coefficients β (Table E1). Since the lowest-situated stone stripes on the Sanetti Plateau are located at an elevation of 3870-3890 m, we used meteorological data (T_{air} and Q_S) from the Tuluka AWS at 3848 m to run the three models. Alternatively, the meteorological data from the higher-situated AWS (Tullu Dimtu and ECWP Station) can be adjusted to the elevation of the stone stripes using a lapse rate of 0.7 °C per 100 m. Running each model with the locally adjusted meteorological data led to the same calculated temperature depression as using the Tuluka AWS data. We rescaled the simulated ground temperatures in 2 cm depth (aggregated to daily values) to the maximum seasonal ground temperature variations in 10 and 50 cm depth observed today to model temperature variations in these depths:

$$T_{\mathrm{50cm,i}} = (\overline{T}_{\mathrm{2cm}} - a) + \frac{(T_{\mathrm{2cm,i}} - min(T_{\mathrm{2cm}})) \times (b - a)}{(max(T_{\mathrm{2cm}}) - min(T_{\mathrm{2cm}}))}, \quad (3)$$

where ($T_{50cm,i}$) are the simulated daily ground temperatures in 50 cm depth in °C ($i = 1,\ldots,n$), ($T_{2cm,i}$) are the aggregated daily ground temperatures in 2 cm depth in °C ($i = 1,\ldots,n$), $\overline{T}_{2cm}$ is the mean air temperature in 2 cm depth in °C, a (= - 1.25 °C) is the predefined seasonal minimum, and b (= 1.25 °C) the predefined maximum of $T_{50cm,i}$. For 10 cm depth (T_{10cm}), a equals to -3 °C and b to 3 °C.

4 Results

4.1 Contemporary ground frost dynamics and phenomena

The Bale Mountains comprise a wide range of periglacial landforms and other characteristic phenomena related to present and relict frost dynamics (Table A1). Contemporary frost phenomena like frozen waterfalls and needle ice as well as active periglacial landforms like patterned grounds and solifluction lobes are limited to the upper part of the valleys (>3900 m), to the Sanetti Plateau, and to the highest peaks. We observed needle ice (3-5 cm long) mainly along water-saturated stream banks at sites with cold air ponding. Needle ice is a typical superficial frost phenomenon in the Bale Mountains related to diurnal freeze-thaw cycles. It forms at clear nights throughout the dry season. Interestingly, we also found evidence for a recurring seasonal frost phenomenon: Up to 10 m high water falls at shaded north-exposed cliffs in the Wasama Valley freeze every year at the beginning of the dry season (i.e. October/November) and persist until the onset of the following rainy season (i.e. February/March). They do not evolve at any other location in the Bale Mountains according to the local guides. Active small-scale polygonal stone nets occur in flat and poorly drained areas on the Sanetti Plateau and unvegetated solifluction lobes can be found above 4100 m on the southern slopes of Mount Wasama (Fig. 3).

The observed present-day ground temperatures in the Bale Mountains show characteristic daily and seasonal variations, but are way off from seasonal or permanent frost conditions (Fig. 4). At the location of the stone stripes on the southern Sanetti Plateau, the mean multiannual ground temperature between the surface and 50 cm depth is 11 °C. On the highest peak Tullu Dimtu, the mean annual ground temperature is 7.5 °C. The mean air temperature at the same location is 2 °C and therefore about 5.5 °C lower than the mean ground temperature. While the daily ground temperature range is largest near the surface and decreases with depth, the seasonal variations at all depths follow a similar cycle (Fig. 4). On the plateau, the ground cools during the dry season and heats up during the wet seasons. The difference between the seasonal minimum and maximum of daily mean ground temperatures over a year is about 10 °C near the surface, 6 °C in 10 cm, and 2.5 °C in 50 cm depth. This shows that seasonal ground temperature variations are also characteristic for tropical mountains with a pronounced diurnal climate.

Near the surface, the diurnal ground temperature amplitude varies on average between 10-20 °C during the rainy and between 20-30 °C during the dry season. Extreme temperatures of up to 45-50 °C during cloudless days and down to -10 °C during clear nights have been observed on the Sanetti Plateau. Nocturnal ground frost on the plateau occurs at 35-90 days per year. However, the frost penetrates only the uppermost centimetres. The diurnal amplitude decreases considerably with increasing depth. At 10 cm depth, temperatures below freezing have not been measured at any of the logger locations during the entire study period. The annual ground temperature profile in the upper 50 cm is relatively constant. The daily temperature difference between the surface and 50 cm depth is rarely larger than ± 2 °C.

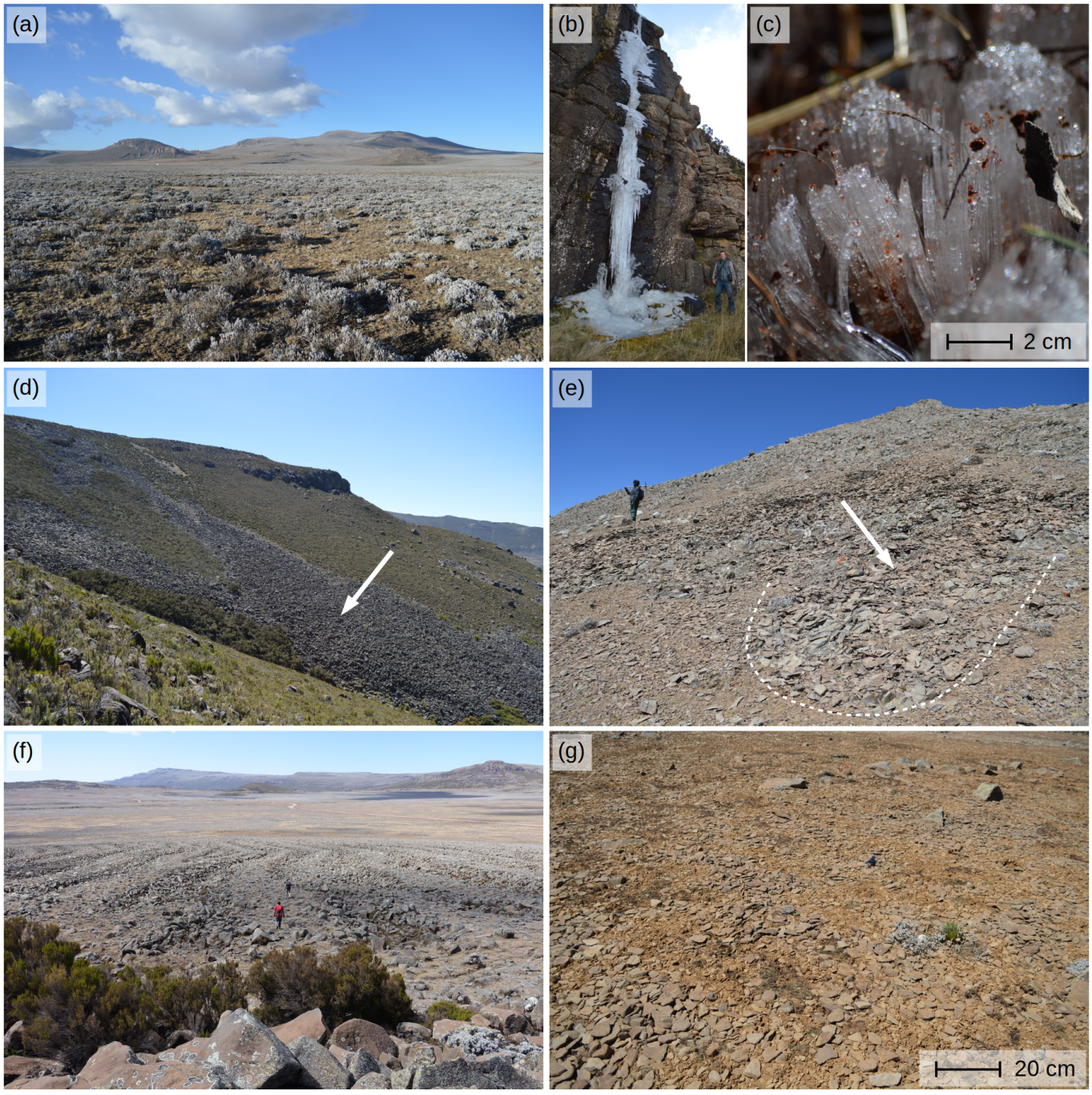

Figure 3. Contemporary frost phenomena and relict periglacial landforms in the Bale Mountains: (a) view from the southern Sanetti Plateau towards Tullu Dimtu, (b) seasonally frozen waterfall and (c) diurnal needle ice in the Wasama Valley, (d) relict blockfields along the southern Harenna Escarpment, (e) active solifluction lobes on Mt. Wasama, (f) relict sorted stone stripes, and (g) active sorted polygons on the Sanetti Plateau.

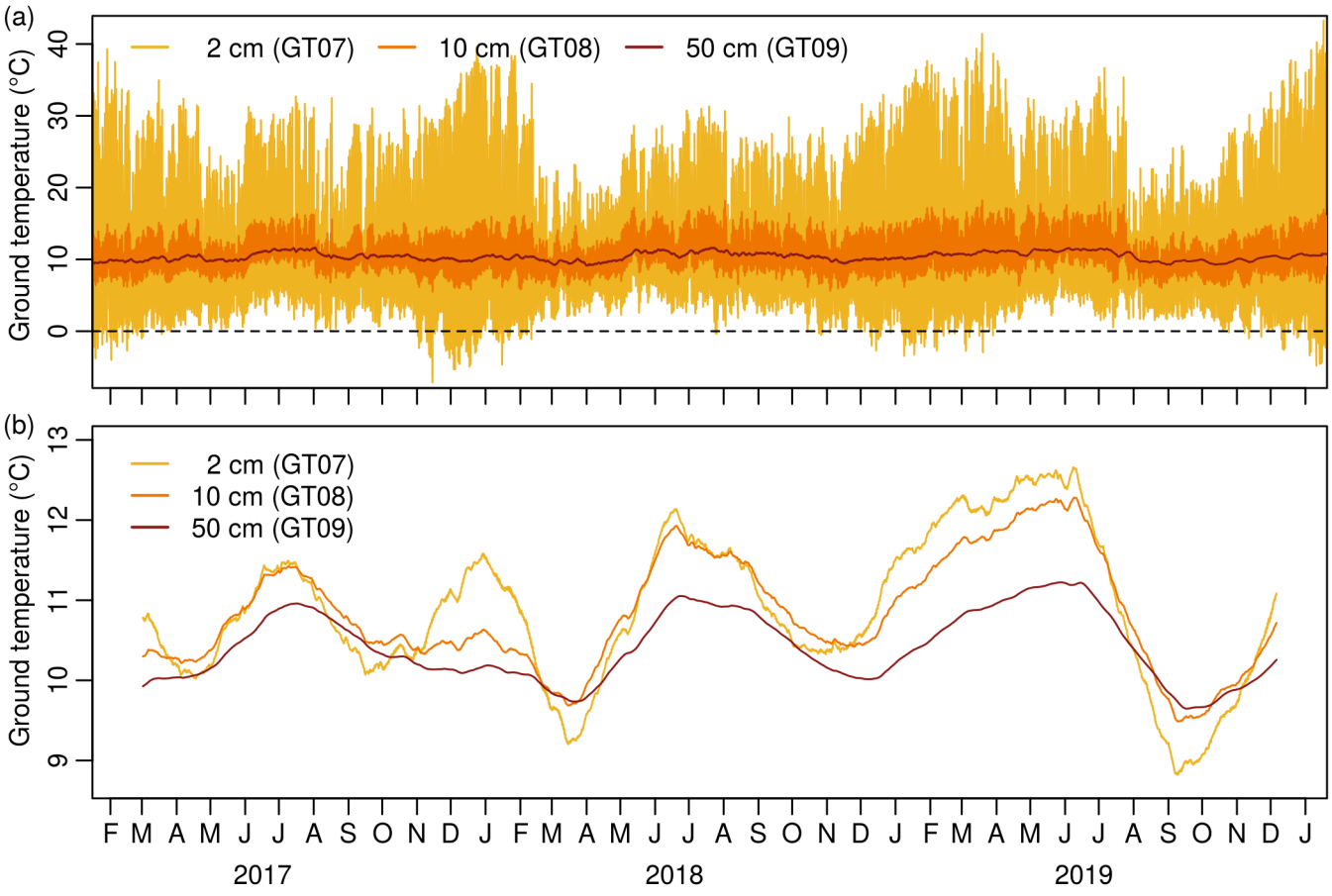

Figure 4. (a) Hourly ground temperatures and (b) seasonal ground temperature variations in 2, 10, and 50 cm depth on the southern Sanetti Plateau (3877 m) from January 2017 to January 2020. A simple moving average with a window size of 91 days was applied to derive seasonal ground temperature variations from hourly measurements. Note that the increase of the seasonal ground temperature amplitude over the measurement period is also confirmed for the other sites on the plateau and is not caused by a shift of the thermistors.

4.2 Characteristics of the relict periglacial landforms

Compared to the modern periglacial processes and landforms, the relict geomorphic features in the Bale Mountains are much larger. Most of the relict periglacial landforms can be found along the Harenna Escarpment, on the Sanetti and Genale Plateau, and on the slopes of the highest peaks (Fig. 5a). Characteristic for the highest peaks of the northern declivity are bare and gentle slopes and the accumulation of coarse scree below heavily eroded basaltic and trachytic cliffs. This type of deposits are likely result of frost wedging in combination with other weathering mechanisms such as thermal stress. The scree slopes differ from the chaotic spread of individual boulders below elongated cliffs at lower elevations. Weathering may still contribute to the development of some of these landforms, but the return of Erica shrubs between the stones as well as the lack of parent

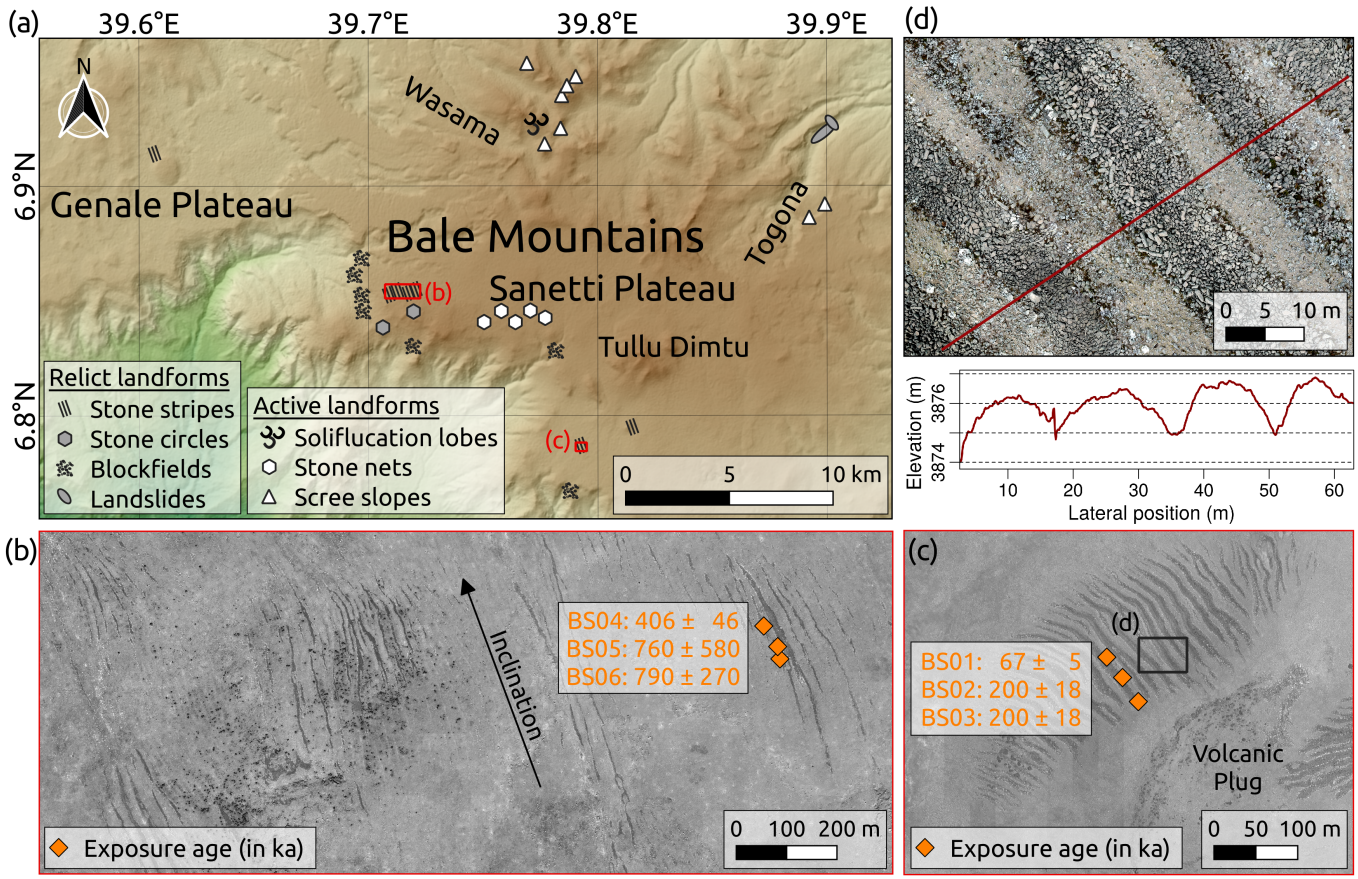

Figure 5. (a) Overview map of relict and active periglacial landforms as well as other characteristic geomorphological features in the Bale Mountains mapped in the field or on high-resolution satellite images. (b) Sorted stone stripes in the western and (c) southern part of the Sanetti Plateau as seen on WorldView-1 satellite images provided by the DigitalGlobe Foundation. The six ^{36}Cl exposure ages were calculated using the Lifton-Sato-Dunai scaling scheme (Lifton et al., 2014; Marrero et al., 2016), are non-erosion corrected, and given in kiloannum (ka) with total uncertainties (1σ). (d) Orthophoto and DSM cross-section profile of the stone stripes derived from the high-resolution UAV data.

material (i.e. cliffs) at some locations indicates that they mainly formed in the past. Another landform associated inter alia with the process of frost weathering are large blockfields located between 3500 and 4000 m on the southern and western declivity of the Sanetti Plateau. The blockfields consist of hardly weathered angular boulders and are no longer active as the presence of lichens and partly reoccupation by Erica shrubs prove. Circular patterns across the Sanetti and Genale Plateau as well as elevated areas of the northern declivity are not further considered here since they are, at least in some areas, of biogenic origin related to the activity of the endemic giant mole-rat (Miehe and Miehe, 1994).

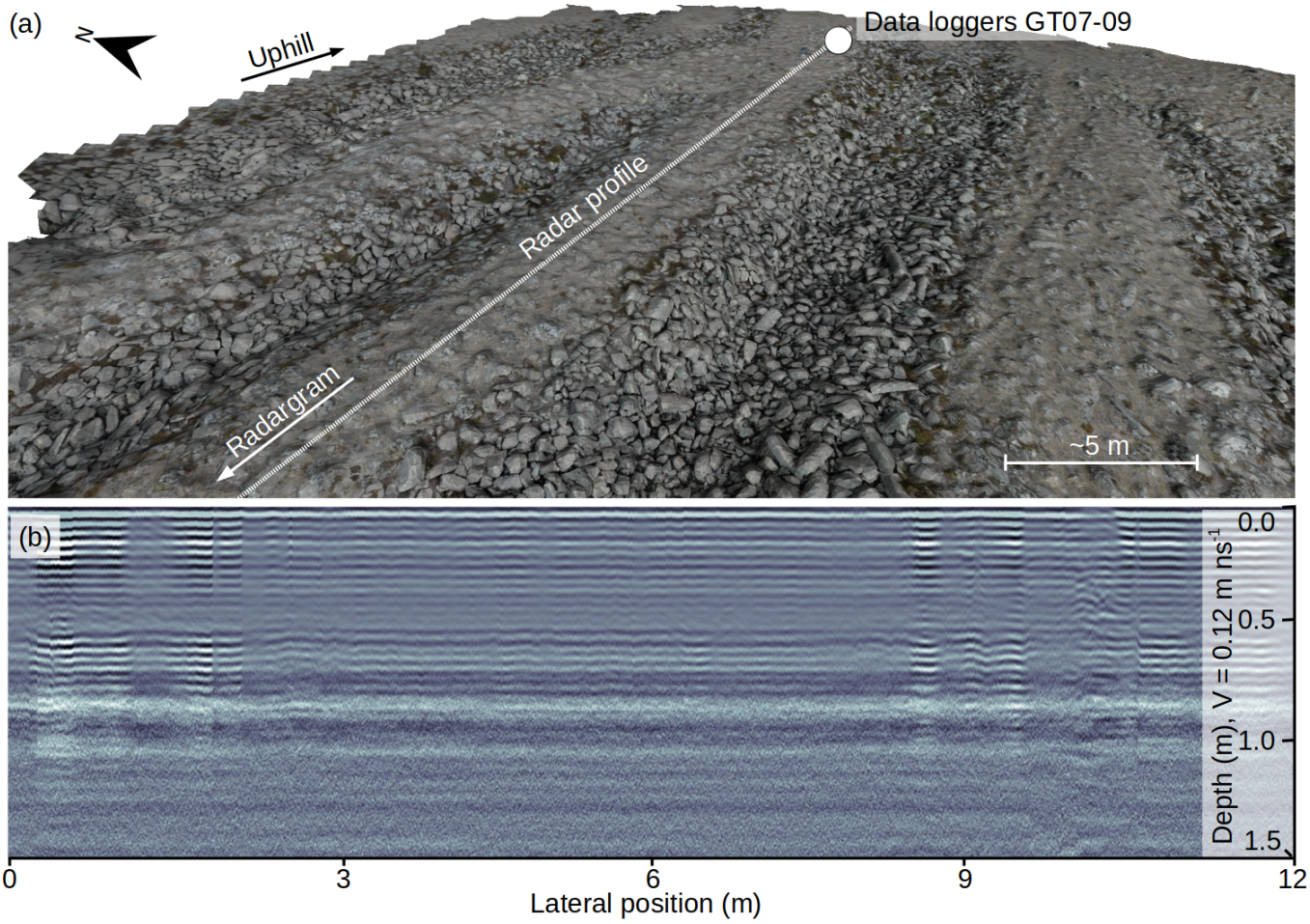

Figure 6. (a) Textured 3D model of the sorted stones stripes on the southern Sanetti Plateau derived from high-resolution UAV data. b) Radargram of a regolith stripe between two coarse stone stripes. For the location of the displayed radargram section (GPR05) see Fig. 1.

The most exceptional geomorphological features on the Sanetti Plateau are large sorted patterned grounds comprising stone circles and stripes. In addition to the known sorted stone stripes on the southern Sanetti Plateau, we also discovered stone stripes on the western Sanetti Plateau and at one site on the lower Genale Plateau (Figs. 5a-c). On the southern Sanetti Plateau and on the Genale Plateau, the stone stripes formed on gentle slopes (inclination: 2 – 9°) of three different volcanic plugs between 3700 and 3950 m. The stone stripes consist of hardly weathered angular or columnar basalt boulders (Figs. 2c and 6a), are partly covered by lichens, and are up to 200 m long, 15 m wide, and 2 m deep as the satellite images and UAV data show (Figs. 5b-d). While the stone stripes are trough-shaped, the areas with finer material inbetween are rampart-like (Fig. 5d). The distance between the stone stripes equals in most cases to the width of the stripes. Typical for some of the stone stripes is that individual narrower branches in the upper part merge downslope to a single wider stripe. As the GPR survey suggests,

the regolith layer between the stone stripes contains no larger rocks (exceeding several decimetres) and is more than 1.5 m deep (Fig. 6b). The surface of the underlying solid rock was not detected. All larger rocks (up to 0.5 m wide and 3 m long) are located mainly in the troughs or on top of the regolith layer as the UAV data underline. On the slightly inclined (2 - 9°) western Sanetti Plateau between 3950 and 4150 m, the stone stripes are 300 – 1000 m long and mainly 5 – 10 m wide (Fig. 5b). Most of the stripes are connected to eroded cliffs. In the upper part, some of the stripes split up into multiple branches. Where the plateau flattens, a transition from sorted stone stripes to less developed stone circles is visible in the field, but hardly recognisable on satellite images.

The six dated rock samples from two different locations on the Sanetti Plateau originate from basaltic (BS01-04) and trachytic (BS05-06) lavaflows as it is indicated by the varying alkali and silica contents (Table C3). We obtained very high ^{36}Cl concentrations, especially for the two trachytic samples (>120 $\times$ 10^6 At g^{-1}) from the western part of the plateau (Table C2). The high ^{36}Cl concentrations translate into non-erosion-corrected surface exposure ages of 67 ± 5, 200 ± 18, and 200 ± 18 ka for the southern and of 406 ± 46, 760 ± 580, and 790 ± 270 ka for the western stone stripes (Table C2). However, due to the high ^{36}Cl concentrations, an erosion rate of >1 mm ka^{-1} or different choice of scaling would alter the exposure ages considerably. The "old" ages conflict with a relatively young formation age (e.g. global LGM or postglacial) as suggested by the morphology and hardly weathered surface of the investigated angular and columnar boulders. Long-term exposure of the sampled rocks to ^{36}Cl-producing cosmic rays prior to or during the formation of the stone stripes could explain this mismatch. Despite the high ^{36}Cl concentrations, a temporary ice cover overlying the stone stripes for several thousand years during the last glacial cycle cannot be entirely ruled out from the exposure dating alone. A meter-thick ice cover would reduce the production rate, but a period of several thousand years would not be sufficient to affect the ^{36}Cl concentrations noticeably or zero the inheritance. However, a temporary ice cover overlying the stripes seems unlikely in light of the absence of any erratic boulders or other glacial landforms near the stripes.

4.3 Modelled ground temperatures and inferred air temperature depression

At the three locations on the Sanetti Plateau (Tullu Dimtu, EWCP Station, and Tuluka), where ground temperatures and a set of meteorological variables were measured simultaneously, ground temperature is mainly controlled by air temperature and global radiation (Fig. E1). The two variables can explain together about 75 ± 3 % of the ground temperature variance (Table E1). Ground temperature and the other meteorological variables do not show any significant linear relationship. This can be explained by the non-consideration of ground moisture. Precipitation, relative humidity, and wind speed affect ground moisture as well as evaporation. Ground moisture and evaporation in turn alter the energy balance at the surface as well as the energy transfer into the ground. However, the correlation between ground temperature and explanatory variables is strong enough to simulate the air temperature depression that corresponds to a MAGT of ca. 0 °C. The diference between the current MAGT at the location of the southern stone stripes and the freezing point is ca. 11 °C. The difference between the seasonal minimum ground temperature and the freezing point is around 9 °C. According to the statistical model, such a MAGT depression would result in a mean air temperature depression of 7.1 ± 1.3 °C (the error is the standard deviation of the three model outputs),

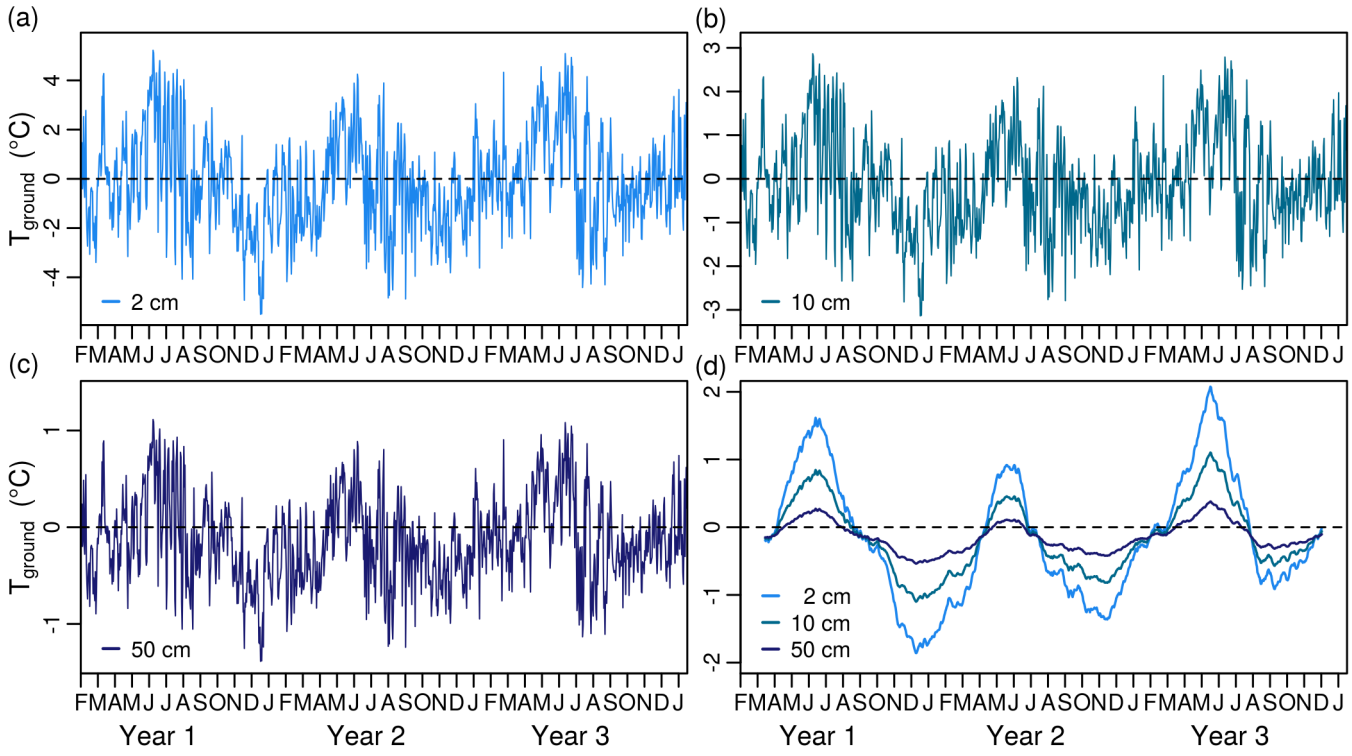

Figure 7. Simulated daily mean ground temperatures in (a) 2 cm, (b) 10 cm, and (c) 50 cm depth on the southern Sanetti Plateau (3877 m) corresponding to a decrease in air temperature of 7.1 ± 1.3 °C and a decrease in global radiation of 30 W/m² relative to the present-day conditions. (d) A simple moving average with a window size of 91 days was applied to derive seasonal ground temperature variations from daily means.

equivalent to a mean annual air temperature on the southern plateau of -1.6 ± 1.4 °C. The deduced stronger decrease of the ground temperature over the air temperature is due to the observed modern statistical relationship. A cooling/warming of the air of 1 °C relates to a decrease/increase of the ground of 1.6-1.9 °C and vice versa (see Table E1 and Fig. E1). The geophysical reasons for this statistical relationship can be manifold. Ground temperature is mainly controlled by radiative forcing and energy exchange between the atmosphere and ground, which in turn is affected by many factors ranging from the temperature, pressure and humidity of the air to the thermal conductivity, specific heat capacity, density, humidity, albedo, etc. of the ground.

Provided that the stone stripes and circles on the Sanetti Plateau formed under periglacial conditions (ground temperatures fluctuating around 0 °C), the occurrence of these features may indicate a past air temperature depression at this elevation in the order of 7.1 ± 1.3 °C. However, it should be noted that changes in ground properties (e.g. modified albedo and thermal conductivity due to snow coverage and frost) would certainly affect the nature of the multiple linear regression models and therefore also the simulation results. The experiment shows that seasonal ground temperature fluctuations near the surface, in

10 cm, and in 50 cm are theoretically large enough to freeze and thaw the upper decimetres of the ground if the MAGT is lowered by 9-11 °C (Fig. 7). Due to the small seasonal ground temperature variations in 50 cm depth, it seems unlikely that much more than the upper half metre of the ground on the Sanetti Plateau would experience seasonal freezing and thawing under cooler climatic conditions unless seasonal variations are stronger than today.

5 Discussion

This study provides a first systematic investigation of the distribution and characteristics of the enigmatic large sorted stone stripes on the central Sanetti Plateau of the tropical Bale Mountains in the southern Ethiopian Highlands. The extensive geomorphological mapping in the field and on satellite images led to the documentation of previously undescribed large sorted stripes on the western Sanetti Plateau and the lower-elevated Genale Plateau. High-resolution UAV data, GPR radargrams, and ^{36}Cl surface exposure ages in combination with ground temperature measurements provide basic information on the geometry, internal structure, and age of the stone stripes as well as on the contemporary frost dynamics on the Sanetti Plateau. In the following discussion i) we compare the stone stripes from the Bale Mountains with similar landforms in other regions, ii) elaborate a conceptual model for their genesis considering the available data and results, and iii) assess the implications of their occurrence for the reconstruction of the palaeoclimate and palaeoenvironment of the Ethiopian Highlands.

5.1 Comparison of the sorted stone stripes with similar landforms in other regions

The large sorted stone stripes on the Sanetti Plateau are an exceptional geomorphic feature as they represent the only known example of large sorted patterned grounds on a tropical mountain. Most examples of sorted stone polygons, nets, and circles with a diameter exceeding several metres originate from the High Arctic (i.e. Alaska, Greenland, Svalbard) (see review of Washburn, 1980). Well-developed relict patterned grounds consisting of clasts with a diameter of at least several decimetres are also documented for several mid-latitude mountains like the Culebra Range (>4000 m; 37 °N) in southern Colorado (Vopata et al., 2006) or the High Sudetes (>1300 m; 50 °N) in Central Europe (Křížek et al., 2019). However, a global compilation and comparison of large sorted patterned grounds and their climatic and environmental setting is lacking in the scientific literature. Sorted stone stripes with a width of up to 15 m and length of up to 1000 m as on the western Sanetti Plateau have even not been reported from the polar regions. The only other location worldwide where stone stripes in the same order of magnitude and larger have been described are the non-volcanic Falkland Islands in the South Atlantic (André et al., 2008).

The vernacular term for extensive blockstreams and stone stripes in the Falkland Islands is “stone runs”. Stone runs cover large parts of the eastern and western island and are connected to quartzite outcrops in the elevated areas (50-700 m). The stone stripes in the Falkland Island show some interesting similarities and differences with the features on the Sanetti Plateau. They occur in clusters on gentle slopes (inclination: 1-10°), are several hundred meters long, several meters wide, consist of large angular blocks (up to 2 m wide and 5 m long), and originate in some cases from eroded ridges and summit areas. As on the Sanetti Plateau, the coarse stone stripes in the Falkland Islands run parallel downslope and alternate with stripes of

fine-grained material of similar width (André et al., 2008). However, the partial emergence of stone stripes from blockfields and downslope transition into vast blockstreams as it is typical for the Falkdland Islands is uncommon for the Bale Mountains where the stripes are restricted to the plateau and the blockfields to the southern and western escarpment. Also the geological (volcanic vs. sedimentary and metamorphic rocks), climatic (continental vs. oceanic), and geographical setting (tropical mountain vs. mid-latitude island) between the Bale Mountains and Falkland Islands differs considerably. Typical for both locations is the coexistence of coarse and fine-grained material (large angular blocks and regolith) and the evidence for glaciations and cooler conditions during the Pleistocene (Clapperton, 1971; Clapperton and Sudgen, 1976; Groos et al., in revision).

The origin and genesis of the stone runs in the Falkland Islands has been discussed controversially over the last one hundred years and numerous theories have been proposed to explain their formation as a result of different interconnected periglacial processes (frost shattering, frost heave, frost sorting, etc.). Based on a literature review and micromorphological analyses, André et al. (2008) come to a more nuanced conclusion and consider the stone runs as complex polygenetic landform. The authors hypothesise that the parent material (blocks and regolith) formed under subtropical or temperate conditions during the Neogene/Palaeogene. They interpret the stone runs as the product of subsequent frost-sorting during the cold stages of the Pleistocene, but the understanding of the physical processes underlying the frost-related sorting of such large clasts is still fragmentary (Aldiss and Edwards, 1999).

5.2 Genesis of the sorted stone stripes

The small number of analogies worldwide and the lack of a cross-section profile complicate the interpretation of the stone stripes on the Sanetti Plateau. Since the Bale Mountains are of volcanic origin, the stone stripes could be interpreted as remains of former lava flows. However, the regular alternation of coarse and fine-grained stripes as well as the loose and random configuration of blocks in the coarse stripes argue against this hypothesis. The coarse stone stripes consist of igneous rocks, but volcanic processes were certainly not involved in the formation of this landform. Although some of the wider stripes resemble river beds, surface runoff can also not explain the stone stripe pattern (e.g. the alternation of coarse and fine stripes as well as the interruption of many stripes on the western plateau, see Fig. 5b). Furthermore, the total area (ca. 100 x 100 m) above the stone stripe slopes on the volcanic plugs (Fig. 5c) seems too small to generate sufficient surface runoff for the formation of up to 15 m wide river beds. Our data and findings suggest that periglacial processes were the main driver of the formation of the stone stripes as we will outline below.

To deduce the underlying mechanisms of the stone stripe genesis, it is important to shortly summarise the characteristics of this landform again. Typical for the stone stripe pattern is the alternation of coarse and fine stripes on gentle slopes. Both coarse and fine stripes are ~5-15 m wide and run parallel to the maximum slope gradient. The high-resolution UAV orthophotos show that the width of the stripes is about 10-20 times larger than the average size of the clasts. Furthermore, the UAV-based DSM reveals that the coarse stripes are trough-shaped and up to 2 m deep (Fig. 6). Boelhouwers et al. (2003) revealed for sorted stone stripes along an altitudinal gradient in the maritime Subantarctic that the up-doming of the fine material between the

coarse stripes increases with elevation due to deeper frost penetration. The deeper frost penetration at higher elevations results in a deeper depths of vertical sorting and, thus, also a greater degree of lateral sorting (Boelhouwers et al., 2003). Another relevant detail of the stone stripes is the downslope convergence of individual branches and smaller stripes to wider single stone stripes (see Fig. 5c). All these observations correspond surprisingly well to the development of frost patterns on slightly inclined slopes after several hundred freeze-thaw cycles as simulated by numerical computer models (see Fig. 8 and Werner and Hallet, 1993; Mulheran, 1994; Kessler et al., 2001; Kessler and Werner, 2003). Such numerical models can reproduce the self-organization of different sorted grounds by varying just a few parameters (mainly stone concentration, hillslope gradient, and degree of lateral confinement) and need about 500 to 1000 freeze-thaw cycles to form similar stripe patterns as found on the southern Sanetti Plateau (Fig. 5c). Less cycles would lead to a more random configuration and more cycles would eliminate the smaller branches and lead to a "perfect" sorting of the stripes (Fig. 8). Assuming downslope displacement rates of 10-50 cm per year (or cycle) for clasts as it is observed for small-scale periglacial features in the tropics (Francou and Bertran, 1997) would require a similar number of cycles (about 400 to 2000) to form the 200 m long stone stripes on the southern plateau.

A precondition for the formation of patterned grounds is cyclic freezing and thawing and the coexistence of larger stones and a frost susceptible ground (Kessler et al., 2001; Kessler and Werner, 2003). Both large blocks and a frost susceptible ground are present on the Sanetti Plateau. A more than 1.5 metre thick regolith layer covers the underlying bedrock of the plateau as indicated by the GPR measurements. Whether the regolith developed over the Pleistocene or during warmer periods before, as suggested for the Falkland Islands (André et al., 2008), remains unclear. The regolith layer is rich in silt and loam (Lemma et al., 2019) and, thus, sufficiently porous to allow capillary action and the formation of ice lenses. The absensce of any larger stones (exceeding several decimetres) in the fine stripes as confirmed by the GPR surveys is indicative of vertical as well as lateral frost sorting. Another indicator for past frost sorting on the Sanetti Plateau is the up-doming of the regolith between the coarse stone stripes (Boelhouwers et al., 2003) as well as the presence of large stone polygons in the highest and even areas of the western plateau (Miehe and Miehe, 1994). How the sorted stone stripes could have evolved from a random configuration of blocks below eroded cliffs in the course of cyclic freezing and thawing of the ground is illustred in Fig. 8.

A central question related to the genesis of the stone stripes is the MAGT and minimum frost penetration depth needed to sort the largest clasts, which are up to 3 m long and certainly weigh between one and two tonnes. Seasonally frozen grounds and sporadic permafrost still exist at some of the highest tropical and subtropical mountains in Africa (Kaser et al., 2004; Vieira et al., 2017). Potential evidence for past sporadic permafrost in the Bale Mountains exists in the northeastern Togona Valley, which was covered by a 8 km long valley glacier during the Late Pleistocene (Groos et al., in revision). During or after deglaciation of the lower part of the valley, two large landslides (0.5 and 1.5 km long; see Fig. 5a) occurred between the ~18 ka and ~15 ka moraine stages and might have been triggered by slope destabilisation due to thawing permafrost. The contemporary ground temperature measurements show that the formation of seasonal or permanent frost to a depth of several decimetres on the Sanetti Plateau would require a decrease of the MAGT in the order of 9-11 °C. According to the simple sta-

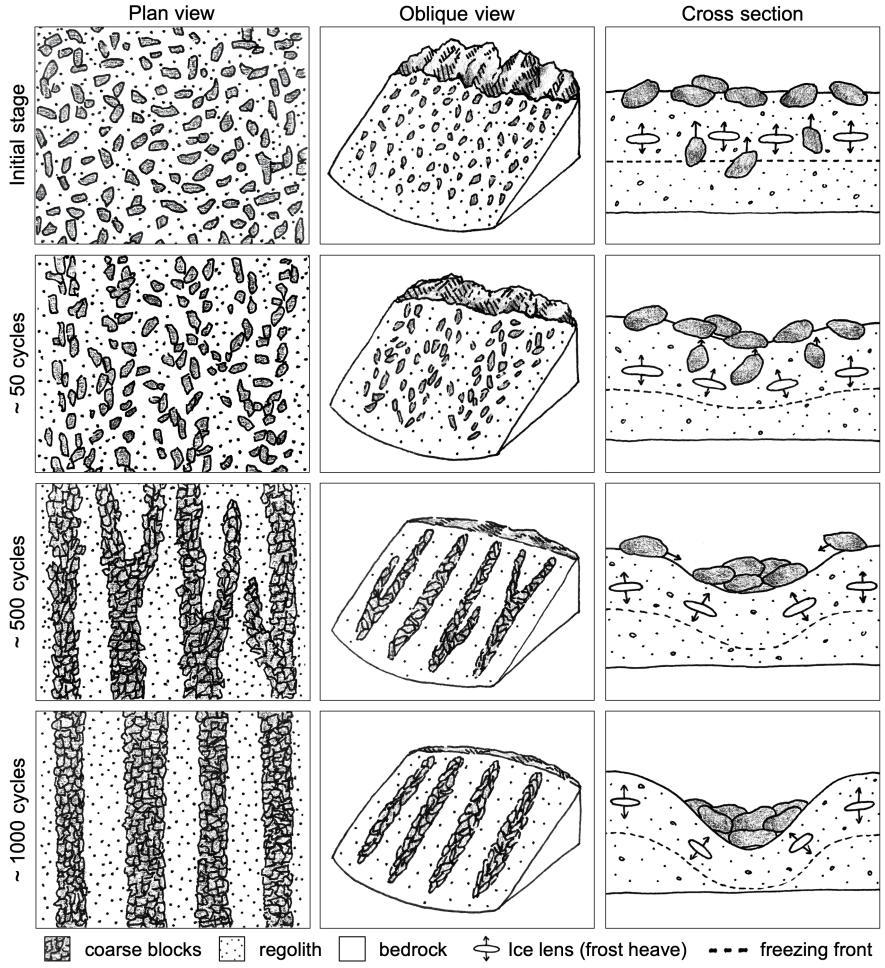

Figure 8. Conceptual model of the genesis of sorted stone stripes on a slightly inclined slope under periglacial conditions. Plan view (downslope orientation towards the bottom of the figure): Stages during the evolution of stone stripes from a random configuration after ~50, ~500, and ~1000 freeze-thaw cycles as simulated by a numerical model that considers lateral frost sorting and the movement of stones along the axis of elongated stone domains (for a detailed model description and the original model outputs see Werner and Hallet, 1993). Note that in the numerical model narrower stripes merge into wider stripes over time. Oblique view: hypothetical stone stripe formation on the Sanetti Plateau below an eroding cliff of a volcanic plug due to cyclic freezing and thawing of the ground. The current status of the self-organisation of stone stripes on the Sanetti Plateau is similar to the configuration in the model after several hundred freeze-thaw cycles. Cross section: principles of the stone stripe formation (although many aspects remain elsuive). In the initial stage the rocks are distributed randomly on the surface and in the fine regolith layer. With the downward penetration of the freezing front (0 °C isotherm) from the surface, ice lenses form and cause vertical frost heave. The recurring formation of ice lenses over time leads to the upfreezing of interior stones and the random movement of blocks on the surface. Randomly formed clusters of blocks are less prone to perturbations than indivual stones or the fine-grained material. The freezing front descends faster in dry and well-drained stone domains than in the wetter fine-grained regolith (which must freeze and be cooled). Since frost expands perpendicular to the freezing front, the stone domain is squezed and blocks are trapped. Blocks in the stone domaine move along the slope gradient and form sorted stripes over time. Drawn by Francesca Andermatt.

tistical model experiment, such a decrease would correspond to an air temperature depression of 7.1 ± 1.3 °C (relative to today).

The coldest and driest period in Africa (ca. 15-45 ka) during the last glacial period (e.g. Tierney et al., 2008) seems the most likely climatic period for a cooling of that magnitude. Between 28-42 ka, an extensive ice cap extending down into the northern valleys covered the Sanetti Plateau. The large stone stripes are located beyond the glacial remains and the assumed maximum extent of the former ice cap (Ossendorf et al., 2019; Groos et al., in revision). One plausible scenario would be the development of the stone stripes in close proximity to the ice cap over several hundred to thousand years due to seasonal freezing and thawing of the ground. Such a scenario would also be plausible for the Falkland Islands, where the stone stripes are located outside the former glacial remains (Clapperton, 1971; Clapperton and Sudgen, 1976). Cool katabatic winds originating from the extensive ice cap on the Sanetti Plateau might have promoted an amplified cooling in the area of the stone stripes. The hardly weathered surface of the stone stripe boulders on the Sanetti Plateau supports a formation during the coldest period of the last glacial cycle, but most of the obtained ^{36}Cl surface exposure ages predate this period. However, it is possible that the exposure ages do not represent the formation or stabilisation age of these features. Since the sampled igneous rocks originate from eroded cliffs and volcanic plugs, they were likely exposed to cosmic radiation prior to (and during) the formation of the stone stripes. Another scenario is the evolution of the stone stripes over several cold stages during the Pleistocene as proposed for the stone runs in the Falkland Islands (Wilson et al., 2008). This would imply the formation of sporadic permafrost during colder periods and the complete thawing of the ground during warmer periods of the Pleistocene. In this case, the stone stripes would have rather formed over several thousand to ten thousand than over a few hundred or thousand years. The exposure ages and high ^{36}Cl would generally support such a scenario.

5.3 The sorted stone stripes as potential climate proxy

The previous analysis provides first evidence that the large sorted stone stripes above 3800-4100 m on the Sanetti Plateau most likely evolved under periglacial conditions during the Pleistocene. Ground temperatures fluctuating around 0 °C and mean annual air temperatures below 0 °C are common for areas where large patterned grounds occur (Goldthwait, 1976; Hallet, 2013). Thus, it is reasonable to assume that a MAGT in the order of 0 °C and a mean annual air temperature smaller 0 °C was a precondition for the genesis of the stone stripes on the Sanetti Plateau. Since the present climatic conditions (the mean annual air tempeature is 5.7 °C at the Tuluka AWS, see Fig. 1) do not support the formation of seasonal or permanent ground frost on the plateau, the existence of these features is an indicator for severe climatic and environmental changes in the Ethiopian Highlands during the Pleistocene. The difference between the present MAGT and freezing point in the order of 11 °C provides a rough estimate for the ground temperature depression during the formation of the stone stripes. Moreover, the statistical model experiment shows that such a decrease of the MAGT would theoretically correspond to an air temperature depression of 7.1 ± 1.3 °C and an absolute mean annual air temperature on the southern plateau of -1.6 ± 1.4 °C. Since the exposure ages generally support a formation of the stone stripes during MIS 2 and 3 as well as over a longer period during the Pleistocene, it is currently not possible to link the inferred high-elevation cooling in the Bale Mountains to a specific climatic period in

tropical Eastern Africa. To corroborate a past regional cooling of that magnitude, further evidence of large patterned grounds or other high-elevation climate proxies from the Ethiopian Highlands would be necessary.

5.4 Future research and outreach

Certain aspects of the genesis and implications of the large sorted stone stripes on the Sanetti Plateau in the Bale Mountains remain unresolved. A key challenge for a better understanding of the palaeoclimate and palaeoenvironment of the Bale Mountains is the development of a robust geochronology. The age of the volcanic plugs, the formation phase of the regolith and stone stripes as well as the termination of the plateau glaciation are relatively uncertain. Additional information on the depth and internal structure (grain size distribution, indicators for cryoturbation, etc.) of the coarse and fine-grained stone stripes would be very useful to gain further insights into the genesis of this landform. Simultaneous ground measurements in the coarse and fine stripes would help to figure out whether the structure of the coarse stone stripes promotes a faster cooling of the ground than the adjacent fine stripes (e.g. Harris and Pedersen, 1998; Juliussen and Humlum, 2008; Wicky and Hauck, 2020).
Since the large sorted stone stripes are a rare and unique geomorphic feature, they represent an important geoheritage site in Ethiopia that complements other geological sites of public iterest such as the Blue Nile Gorge or the active basaltic shield volcano Erta Ale (Williams, 2020). The stone stripes are located in the centre of the Bale Mountains National Park. Some of these features are accessible via dirt road. Hence, the sorted stone stripes may be another suitable destination for geotourism in the park.

6 Conclusions

This contribution provides a first systematic investigation of contemperorary small-scale frost phenomena and relict large sorted stone stripes on the more than 4000 m high central Sanetti Plateau of the Bale Mountains in the tropical Ethiopian Highlands. The coarse stone stripes on the slightly inclined Sanetti Plateau, which alternate with fine regolith stripes, are an exceptional geomorphic feature as they consist of very large clasts (up to 3 m long) and are up to 2 m deep, 15 m wide, and 1000 m long. Moreover, these features are enigmatic in a way that patterned grounds exceeding several metres have yet only been reported from the mid-latitudes and polar regions, but not from the tropics. The detailed analysis of the stone stripes' geometry and internal structure based on UAV and GPR surveys reveals an up-doming of the fine regolith stripes, a lack of larger clasts inside the fine regolith stripes, and a downslope convergence of individual narrower stone stripes and branches into single wider stone stripes. All these details suggest lateral and vertical sorting in the course of cyclic freezing and thawing of the ground as main mechanism for the genesis of the stone stripes from an intial random configuration of blocks below eroded cliffs. Superficial nocturnal ground frost occurs frequently on the Sanetti Plateau, but the ground below the upper few centimetres remains unfrozen the entire year. The measured ground temperatures suggest a mean annual ground temperature depression of about 11 °C for the formation of seasonal or permanent frost, corresponding to an air temperature decrease of about 6-8 °C (relative to today). Two different scenarios are plausible for the genesis of the stone stripes and are in principle supported by the exposure ages. Either they formed in proximity of the former ice cap on the Sanetti Plateau due to seasonal frost heave and

sorting during the last glacial cycle or they developed over multiple cold phases of the Pleistocene. Although certain aspects of the genesis of the large sorted stone stripes remain elusive, the presence of these geomorphic features provides independent evidence besides the glacial landforms for unprecedented palaeoclimatic and palaeoenvironmental changes in the tropical Bale Mountains during the Pleistocene.

Data availability. Ground temperature data, meteorological data, UAV data, GPR data as well as additional field photos of the stone stripes are available upon request by email to the corresponding author.

Author contributions. ARG, NA, and HV designed the research concept, conducted the geomorphological mapping, sampled the stone stripes for exposure dating, and installed the ground temperature data loggers. ARG and NA processed the rock samples in the laboratory. FH set up the weather stations. LW conducted the GPR measurements and serviced the weather stations. FH, LW, and TN processed and provided the meteorological data. ARG and JN processed the ground temperature data, conducted the statistical analysis, and performed the ground temperature simulations. ARG drafted the manuscript and figures with contributions from all authors.

Competing interests. The authors declare that they have no conflict of interest.

Acknowledgements. This research was funded by the Swiss National Science Foundation (SNF, grant no. 200021E-165446/1) and the German Research Foundation (DFG) in the framework of the joint Ethio-European DFG Research Unit 2358 “The Mountain Exile Hypothesis”. We thank the Ethiopian Wildlife Conservation Authority, the College of Natural and Computational Sciences (Addis Ababa University), the Department of Plant Biology and Biodiversity Management (Addis Ababa University), the Philipps University Marburg, the Frankfurt Zoological Society, the Ethiopian Wolf Project, and the Bale Mountains National Park for their cooperation and kind permission to conduct field work. We are grateful to Mekbib Fekadu, Wege Abebe, Katinka Thielsen, Tiziana Koch, Aschalew Gashaw, Terefe Endale, Geremew Mebratu, Beriso Kemal, Mohammed Kedir, Edris Abduku, Sabrina Erlwein, Lukas Munz, Julian Struck, and Bruk Lemma for contributing to the preparation and implementation of the field work, Serdar Yesilyurt for support in the lab, Francesca Andermatt for drawing the conceptual model, and Armin Rist for the fruitful discussion. Special thanks also go to the DigitalGlobe Foundation for providing high-resolution WorldView-1 satellite images of the Bale Mountains (granted to ARG) and to the developers/maintainers of the free and open-source software used in this study (R, QGIS, OpenDroneMap, MeshLab, LibreOffice, etc.).

Appendix A: Catalogue of periglacial landforms

Table A1. Overview of periglacial landforms and other characteristic geomorphological features in the Bale Mountains mapped in the field and on satellite images. A compilation of glacial landforms in the Bale Mountains is provided by Groos et al. (in revision).

ID	Landform / Feature	Status	Latitude (°N)	Longitude (°E)	Elevation (m)	Slope (°)	Aspect (°)
1	Sorted stone nets	active	6.84253	39.77714	4110 – 4140	0	–
2	Scree slope	active	6.92509	39.78395	3930 – 4090	18 – 37	110 – 120
3	Solifluction lobes	active	6.92699	39.77194	4130 – 4190	20 – 22	150 – 170
4	Sorted stone stripes	relict	6.78692	39.79278	3865 – 3880	3 – 9	290 – 70
5	Sorted stone stripes	relict	6.79496	39.81503	3880 – 3940	3 – 7	70 – 180
6	Sorted stone stripes	relict	6.85486	39.72071	4020 – 4100	2 – 9	330 – 350
7	Sorted stone stripes	relict	6.85336	39.71750	4020 – 4140	2 – 9	330 – 350
8	Sorted stone stripes	relict	6.85432	39.71263	4000 – 4070	2 – 9	330 – 350
9	Sorted stone stripes	relict	6.85264	39.70884	3940 – 4100	2 – 9	330 – 350
10	Sorted stone stripes	relict	6.91414	39.60676	3715 – 3730	2 – 9	270 – 290
11	Sorted stone polygons	relict	6.83843	39.70631	4000 – 4100	0 – 4	180 – 200
12	Sorted stone polygons	relict	6.84533	39.71969	4120 – 4170	0 – 4	330 – 350
13	Blockfield	relict	6.76713	39.78794	3690 – 3800	19 – 25	240 – 250
14	Blockfield	relict	6.82818	39.78168	3970 – 4030	12 – 15	260 – 270
15	Blockfield	relict	6.83016	39.71949	3700 – 3940	17 – 19	200 – 220
16	Blockfield	relict	6.84541	39.69772	3800 – 3880	9 – 11	300 – 310
17	Blockfield	relict	6.85245	39.69704	3700 – 3830	12 – 14	260 – 270
18	Blockfield	relict	6.86119	39.69388	3550 – 3820	20 – 24	250 – 270
19	Blockfield	relict	6.86848	39.69701	3600 – 3880	20 – 24	320 – 330
20	Scree slope	relict	6.89194	39.89919	3890 – 3940	20 – 23	300 – 320
21	Scree slope	relict	6.88617	39.89236	3930 – 3980	20 – 26	350 – 360
22	Scree slope	relict	6.91829	39.77699	4070 – 4110	24 – 25	350 – 360
23	Scree slope	relict	6.95343	39.76925	4045 – 4065	24 – 25	290 – 310
24	Scree slope	relict	6.93937	39.78443	4080 – 4110	21 – 25	290 – 310
25	Scree slope	relict	6.94363	39.78672	4055 – 4100	23 – 25	350 – 360
26	Scree slope	relict	6.94764	39.79058	4080 – 4150	24 – 27	10 – 20
27	Landslide	relict	6.92268	39.89833	3490 – 3720	2 – 30	60 – 70
28	Landslide	relict	6.92644	39.90251	3490 – 3650	2 – 40	160 – 170

Appendix B: GPR system settings

Table B1. System settings of the used Pulse EKKO PRO GPR.

Setting type	Setting	Setting type	Setting	Setting type	Setting
Frequency:	1000 MHz	Survey type:	Reflection	Start offset:	0 m
Time window:	30 ns (1.6 m)	Step size:	0.010 m	GPR trigger:	Odometer
Sampling Interval:	Normal (100 ps)	Calibration:	1080.0	Antenna separation:	0.15 m
Stacks:	4	Transmitter:	pE Pro Auto	Antenna polarization:	broadside
Velocity:	0.12 m ns^{-1}	Receiver:	pulseEKKO Pro	Antenna orientation:	Perpendicular

Appendix C: Cosmogenic ^{36}Cl data

Table C1. Description of periglacial features on the Sanetti Plateau sampled for ^{36}Cl surface exposure dating.

Rock sample	Lithology	Latitude (°N)	Longitude (°E)	Elevation (m a.s.l.)	Boulder length (m)	Boulder width (m)	Boulder height (m)	Sample thickness (cm)	Shielding factor
BS01	Basalt	6.78634	39.79297	3874	2.1	0.6	1.0	2.5	0.9961
BS02	Basalt	6.78660	39.79280	3869	1.5	0.5	1.4	4.5	0.9961
BS03	Basalt	6.78682	39.79263	3865	0.6	0.4	1.0	3.0	0.9997
BS04	Basalt	6.85491	39.72078	4050	0.8	0.6	1.1	5.0	0.9990
BS05	Trachyandesite	6.85513	39.72074	4049	0.5	0.5	1.0	4.5	0.9990
BS06	Trachyandesite	6.85550	39.72049	4045	1.5	0.5	0.6	3.5	0.9994

Data from Groos et al. (in revision).

Table C2. Cosmogenic ^{36}Cl data and surface exposure ages of the rock samples from the Sanetti Plateau.

Rock sample	Rock dissolved (g)	^{35}Cl Spike (mg)	Cl (ppm)	^{36}Cl (10^5 At g^{-1})	Exposure age (ka)*	Exposure age (ka)**	Exposure age (ka)***
BS01	30.0307	2.5682	20.7 ± 0.08	30.44 ± 0.82	66.5 ± 4.5	68.2 ± 5.2	70.8 ± 5.9
BS02	30.0068	2.5584	31.5 ± 0.07	85.93 ± 1.63	200.0 ± 18.0	221.0 ± 25.0	282.0 ± 46.0
BS03	29.9887	2.5584	29.1 ± 0.04	85.66 ± 2.45	200.0 ± 18.0	221.0 ± 26.0	283.0 ± 46.0
BS04	29.9982	2.5652	40.9 ± 0.22	153.56 ± 2.58	406.0 ± 46.0	580.0 ± 180.0	–
BS05	30.0349	2.5719	1027.6 ± 11.19	1268.53 ± 25.03	760.0 ± 580.0	510.0 ± 270.0	–
BS06	30.0705	2.5682	1228.0 ± 13.43	1394.82 ± 46.40	790.0 ± 270.0	500.0 ± 300.0	–

Data from Groos et al. (in revision). *Erosion rate = 0 mm ka^{-1}. **Erosion rate = 1 mm ka^{-1}. ***Erosion rate = 2 mm ka^{-1}

Table C3. Major and trace element data of the six rock samples from the Sanetti Plateau.

Rock sample	O *	C *	Na *	Mg *	Al *	Si *	P *	K *	Ca *	Ti *	Mn *	Fe *	B **	Sm **	Gd **	U **	Th **
BS01	57.88	5.13	1.74	5.61	7.40	21.97	0.09	0.62	7.86	1.44	0.15	9.10	3	3.3	3.6	0.3	1.1
BS02	56.64	5.09	1.70	5.50	7.23	21.13	0.14	0.61	7.90	1.41	0.15	9.13	11	3.8	4.1	0.3	1.3
BS03	56.17	4.98	1.68	5.23	7.52	20.90	0.15	0.60	8.00	1.44	0.14	8.97	12	3.8	4.1	0.3	1.2
BS04	54.79	3.85	2.50	3.56	8.30	22.86	0.14	0.81	6.96	1.42	0.15	8.81	6	4.3	4.4	0.4	1.7
BS05	47.82	0.68	5.01	0.21	9.09	28.42	0.05	3.59	1.92	0.24	0.19	4.39	1	6.4	4.8	2.9	14.8
BS06	46.47	0.66	5.16	0.18	9.42	26.99	0.05	3.64	1.90	0.24	0.19	4.41	15	6.7	4.9	1.9	15.5

Data from Groos et al. (in revision). *Unit = % w/w. **Unit = ppm.

Appendix D: Weather stations and ground temperature data loggers

Table D1. Overview of the ground temperature data loggers installed on the Sanetti Plateau.

Data logger	Latitude (°N)	Longitude (°E)	Elevation (m a.s.l.)	Depth (cm)	Slope (°)	Aspect (°)	Start of measurement	Readout dates
GT07	6.78665	39.79342	3877	2 ± 1	8	320	21.01.17	10.12.17, 06.01.18, 25.01.20
GT08	6.78665	39.79342	3877	10 ± 2	8	320	21.01.17	10.12.17, 06.01.18, 25.01.20
GT09	6.78665	39.79342	3877	50 ± 5	8	320	21.01.17	10.12.17, 06.01.18, 25.01.20
GT10	6.79474	39.81469	3932	2 ± 1	10	130	21.01.17	11.12.17, 06.01.18, 26.01.20
GT11	6.79474	39.81469	3932	10 ± 2	10	130	21.01.17	11.12.17, 06.01.18, 26.01.20
GT12	6.79474	39.81469	3932	50 ± 5	10	130	21.01.17	11.12.17, 06.01.18, 26.01.20
GT13	6.82617	39.81897	4377	2 ± 1	0	-	21.01.17	19.12.17, 20.01.20, 26.01.20
GT14	6.82617	39.81897	4377	10 ± 2	0	-	21.01.17	19.12.17, 20.01.20
GT15	6.82617	39.81897	4377	50 ± 5	0	-	21.01.17	19.12.17, 26.01.20
TM04	6.84411	39.87876	4129	2 ± 1	0	-	18.01.17	09.12.17, 05.01.18, 10.06.18
TM08	6.82617	39.81897	4377	2 ± 1	0	-	21.01.17	19.12.17
TM09	6.86644	39.74365	4084	2 ± 1	0	-	23.01.17	12.12.17, 15.06.18, 24.01.20
TM10	6.85509	39.71345	4022	2 ± 1	0	-	23.01.17	13.12.17, 15.06.18, 24.01.20

Table D2. Overview of the automatic weather stations installed on the Sanetti Plateau.

Weather station	Location	Latitude (°N)	Longitude (°E)	Elevation (m a.s.l.)	First measurement	Last measurement	Data completeness (%)*
BALE001	Tullu Dimtu	6.82693	39.81871	4377	04.02.17	31.01.20	73
BALE002	Tuluka	6.78945	39.77511	3848	02.02.17	30.01.20	100
BALE009	EWCP Station	6.84945	39.88197	4124	01.02.17	30.01.20	100

*Ratio of actual to maximum possible measurements during the respective measurement period.

Appendix E: Ground temperature model

Table E1. Coefficients and goodness of fit of the three established multiple linear regression models (MLRM) with ground temperature as dependent and air temperature and global radiation as explanatory variables. Distance means the distance between AWS and ground temperature data logger, β_0 is the intercept, β_1 the air temperature coefficiet, and β_2 the incoming shortwave radiation coefficient.

Linear regression model	Elevation (m)	Distance (m)	β_0	β_1	β_2	R² cal	RMSE cal (°C)	R² val	RMSE val (°C)
MLRM Tullu Dimtu	4377	90	3.7	1.7	0.004	0.73	3.0	0.72	3.0
MLRM EWCP Station	4124	690	1.2	1.6	0.010	0.79	3.6	0.76	3.6
MLRM Tuluka	3848	2050	-0.5	1.9	0.004	0.63	4.9	0.78	4.0

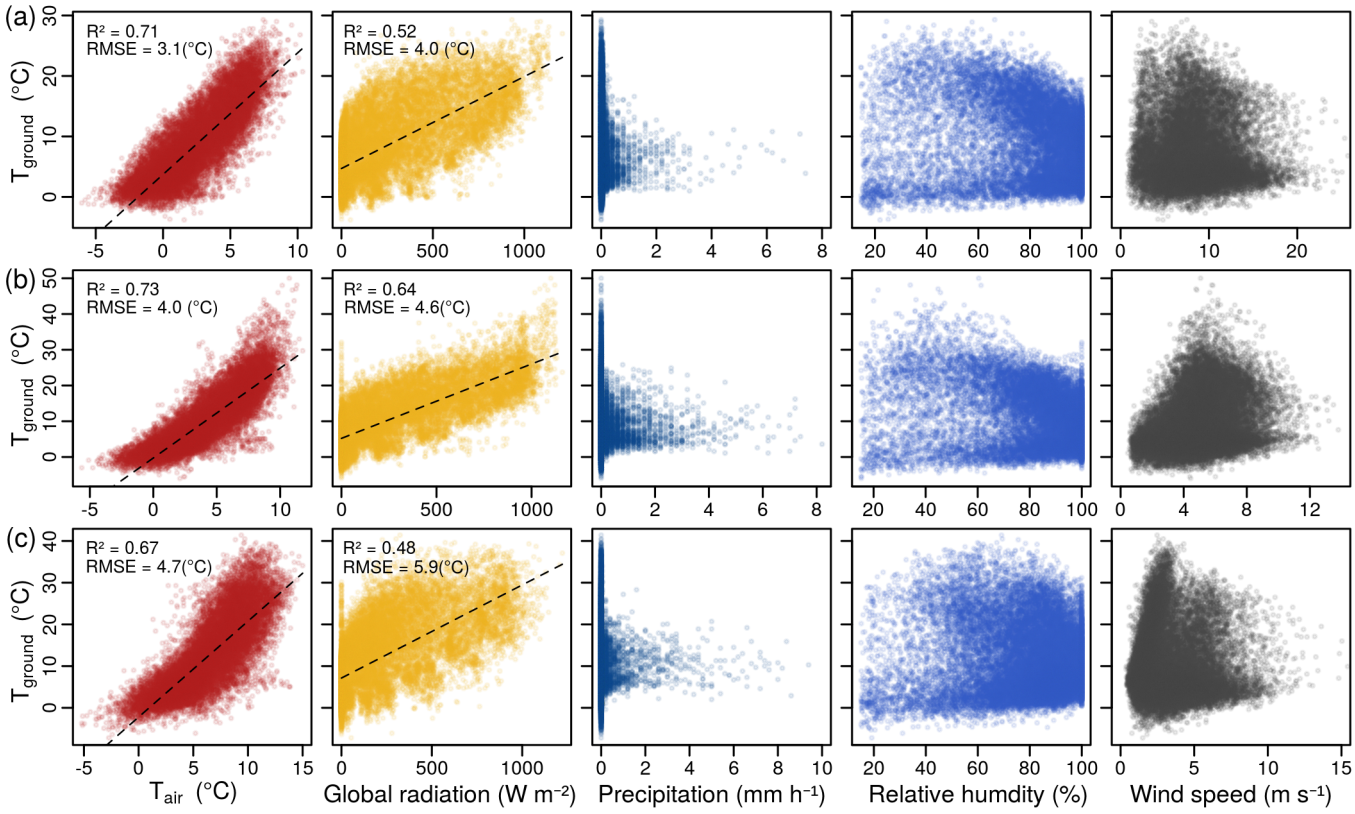

Figure E1. Correlation between hourly ground temperatures in 2 cm depth and different meteorological variables at three different locations: (a) Tullu Dimtu (GT13 vs. BALE001), (b) EWCP Station (TM04 vs. BALE009), (c) Tuluka (GT07 vs. BALE002).

References

Aldiss, D. T. and Edwards, E. J.: The Geology of the Falkdland Islands, British Geological Survey Technical Report WC/99110, 1999.

André, M.-F., Hall, K., Bertran, P., and Arocena, J.: Stone Runs in the Falkland Islands: Periglacial or Tropical?, Geomorphology, 95, 524–543, https://doi.org/10.1016/j.geomorph.2007.07.006, 2008.

Ball, D. F. and Goodier, R.: Large Sorted Stone-Stripes in the Rhinog Mountains, North Wales, Geogr. Ann. Ser. A-phys. Geogr., 50, 54, https://doi.org/10.2307/520871, 1968.

Balme, M., Gallagher, C., Page, D., Murray, J., and Muller, J.-P.: Sorted Stone Circles in Elysium Planitia, Mars: Implications for Recent Martian Climate, Icarus, 200, 30–38, https://doi.org/10.1016/j.icarus.2008.11.010, 2009.

Barrows, T., Stone, J. O., and Fifield, L. K.: Exposure Ages for Pleistocene Periglacial Deposits in Australia, Quat. Sci. Rev., 23, 697–708, https://doi.org/10.1016/j.quascirev.2003.10.011, 2004.

Bertran, P., Klaric, L., Lenoble, A., Masson, B., and Vallin, L.: The Impact of Periglacial Processes on Palaeolithic Sites: The Case of Sorted Patterned Grounds, Quat. Int., 214, 17–29, https://doi.org/10.1016/j.quaint.2009.10.021, 2010.

Boelhouwers, J., Holness, S., and Sumner, P.: The Maritime Subantarctic: A Distinct Periglacial Environment, Geomorphology, 52, 39–55, https://doi.org/10.1016/S0169-555X(02)00247-7, 2003.

Chandler, B. M., Lovell, H., Boston, C. M., Lukas, S., Barr, I. D., Benediktsson, Í. Ö., Benn, D. I., Clark, C. D., Darvill, C. M., Evans, D. J., Ewertowski, M. W., Loibl, D., Margold, M., Otto, J.-C., Roberts, D. H., Stokes, C. R., Storrar, R. D., and Stroeven, A. P.: Glacial Geomorphological Mapping: A Review of Approaches and Frameworks for Best Practice, Earth-Sci. Rev., 185, 806–846, https://doi.org/10.1016/j.earscirev.2018.07.015, 2018.

Clapperton, C. M.: Evidence of Cirque Glaciation in the Falkdland Islands, J. Glaciol., 10, 121–125, https://doi.org/10.3189/S0022143000013058, 1971.

Clapperton, C. M. and Sudgen, D. E.: The Maximum Extent of Glaciers in Part of West Falkland, J. Glaciol., 17, 73–77, https://doi.org/10.3189/S0022143000030732, 1976.

Conway, D.: The Climate and Hydrology of the Upper Blue Nile River, Geogr. J., 166, 49–62, https://doi.org/10.1111/j.1475-4959.2000.tb00006.x, 2000.

Costa, K., Russell, J., Konecky, B., and Lamb, H.: Isotopic Reconstruction of the African Humid Period and Congo Air Boundary Migration at Lake Tana, Ethiopia, Quat. Sci. Rev., 83, 58–67, https://doi.org/10.1016/j.quascirev.2013.10.031, 2014.

de Deus Vidal Junior, J. and Clark, R. V.: Afro-Alpine Plant Diversity in the Tropical Mountains of Africa, Encyclopedia of the World's Biomes, pp. 1–22, https://doi.org/10.1016/B978-0-12-409548-9.11885-8.

Francou, B. and Bertran, P.: A Multivariate Analysis of Clast Displacement Rates on Stone-banked Sheets, Cordillera Real, Bolivia, Permafrost and Periglacial Process., 8, 12, 1997.

Francou, B., Méhauté, N. L., and Jomelli, V.: Factors Controlling Spacing Distances of Sorted Stripes in a Low-Latitude, Alpine Environment (Cordillera Real, 16 °S, Bolivia): Spacing Distances of Sorted Stripes in the Cordillera Real, Permafrost Periglacial Process., 12, 367–377, https://doi.org/10.1002/ppp.398, 2001.

Galloway, R. W.: Late Quaternary Climates in Australia, J. Geol., 73, 603–618, https://doi.org/10.1086/627096, 1965.

Gebrechorkos, S. H., Hülsmann, S., and Bernhofer, C.: Long-Term Trends in Rainfall and Temperature Using High-Resolution Climate Datasets in East Africa, Sci. Rep., 9, 1–9, https://doi.org/10.1038/s41598-019-47933-8, 2019.

Gindraux, S., Boesch, R., and Farinotti, D.: Accuracy Assessment of Digital Surface Models from Unmanned Aerial Vehicles' Imagery on Glaciers, Remote Sens., 9, 1–15, https://doi.org/10.3390/rs9020186, 2017.

Goldthwait, R. P.: Frost Sorted Patterned Ground: A Review, Quat. Res., 6, 27–35, 1976.

Grab, S.: Glacial and Periglacial Phenomena in Ethiopia: A Review, Permafrost Periglacial Process., 13, 71–76, https://doi.org/10.1002/ppp.405, 2002.

Groos, A. R., Bertschinger, T. J., Kummer, C. M., Erlwein, S., Munz, L., and Philipp, A.: The Potential of Low-Cost UAVs and Open-Source Photogrammetry Software for High-Resolution Monitoring of Alpine Glaciers: A Case Study from the Kanderfirn (Swiss Alps), Geosciences, 9, 1–21, https://doi.org/10.3390/geosciences9080356, 2019.

Groos, A. R., Akçar, N., Yesilyurt, S., Miehe, G., Vockenhuber, C., and Veit, H.: Non-uniform Late Pleistocene glacier fluctuations in tropical Eastern Africa, Science Advances, in revision.

Hallet, B.: Stone Circles: Form and Soil Kinematics, Proc. R. Soc. A, 371, 20120 357, https://doi.org/10.1098/rsta.2012.0357, 2013.

Hallet, B., Sletten, R., and Whilden, K.: Micro-Relief Development in Polygonal Patterned Ground in the Dry Valleys of Antarctica, Quat. res., 75, 347–355, https://doi.org/10.1016/j.yqres.2010.12.009, 2011.

Harris, S. A. and Pedersen, D. E.: Thermal Regimes beneath Coarse Blocky Materials, Permafrost Periglac. Process., 9, 107–120, 1998.

Hedberg, O.: Vegetation belts of East African Mountains, Svensk bot Tidskr, 45, 140–202, 1951.

Hendrickx, H., Jacob, M., Frankl, A., Guyassa, E., and Nyssen, J.: Quaternary Glacial and Periglacial Processes in the Ethiopian Highlands in Relation to the Current Afro-Alpine Vegetation, Z. Geomorphol., 59, 37–57, https://doi.org/10.1127/0372-8854/2014/0128, 2014.

Ivy-Ochs, S., Synal, H.-A., Roth, C., and Schaller, M.: Initial Results from Isotope Dilution for Cl and 36Cl Measurements at the PSI/ETH Zurich AMS Facility, Nucl. Instrum. Methods Phys. Res. B, 223-224, 623–627, https://doi.org/10.1016/j.nimb.2004.04.115, 2004.

Ivy-Ochs, S., Kerschner, H., Maisch, M., Christl, M., Kubik, P. W., and Schlüchter, C.: Latest Pleistocene and Holocene Glacier Variations in the European Alps, Quat. Sci. Rev., 28, 2137–2149, https://doi.org/10.1016/j.quascirev.2009.03.009, 2009.

James, M. R. and Robson, S.: Mitigating Systematic Error in Topographic Models Derived from UAV and Ground-Based Image Networks, Earth Surf. Process. Landf., 39, 1413–1420, https://doi.org/10.1002/esp.3609, 2014.

Juliussen, H. and Humlum, O.: Thermal Regime of Openwork Block Fields on the Mountains Elgåhogna and Sølen, Central-Eastern Norway, Permafrost Periglac. Process., 19, 1–18, https://doi.org/10.1002/ppp.607, 2008.

Kaser, G., Hardy, D. R., Mölg, T., Bradley, R. S., and Hyera, T. M.: Modern Glacier Retreat on Kilimanjaro as Evidence of Climate Change: Observations and Facts, Int. J. Climatol., 24, 329–339, https://doi.org/10.1002/joc.1008, 2004.

Kessler, M. A. and Werner, B. T.: Self-Organization of Sorted Patterned Ground, Science, 299, 380–383, https://doi.org/10.1126/science.1077309, 2003.

Kessler, M. A., Murray, A. B., Werner, B. T., and Hallet, B.: A Model for Sorted Circles as Self-Organized Patterns, J. Geophys. Res., 106, 13 287–13 306, https://doi.org/10.1029/2001JB000279, 2001.

Křížek, M., Krause, D., Uxa, T., Engel, Z., Treml, V., and Traczyk, A.: Patterned Ground above the Alpine Timberline in the High Sudetes, Central Europe, J. Maps, 15, 563–569, https://doi.org/10.1080/17445647.2019.1636890, 2019.

Lemma, B., Mekonnen, B., Glaser, B., Zech, W., Nemomissa, S., Bekele, T., Bittner, L., and Zech, M.: Chemotaxonomic Patterns of Vegetation and Soils along Altitudinal Transects of the Bale Mountains, Ethiopia, and Implications for Paleovegetation Reconstructions – Part II: Lignin-Derived Phenols and Leaf-Wax-Derived n-Alkanes, E&G Quaternary Sci. J., 68, 189–200, https://doi.org/10.5194/egqsj-68-189-2019, 2019.

Lemma, B., Kebede Gurmessa, S., Nemomissa, S., Otte, I., Glaser, B., and Zech, M.: Spatial and Temporal ^{2}H and ^{18}O Isotope Variation of Contemporary Precipitation in the Bale Mountains, Ethiopia, Isot. Environ. Health Stud., pp. 1–14, https://doi.org/10.1080/10256016.2020.1717487, 2020.

Levin, N. E., Zipser, E. J., and Cerling, T. E.: Isotopic Composition of Waters from Ethiopia and Kenya: Insights into Moisture Sources for Eastern Africa, J. Geophys. Res., 114, 1–13, https://doi.org/10.1029/2009JD012166, 2009.

Lifton, N., Sato, T., and Dunai, T. J.: Scaling in Situ Cosmogenic Nuclide Production Rates Using Analytical Approximations to Atmospheric Cosmic-Ray Fluxes, Earth Planet. Sci. Lett., 386, 149–160, https://doi.org/10.1016/j.epsl.2013.10.052, 2014.

Mangold, N.: High Latitude Patterned Grounds on Mars: Classification, Distribution and Climatic Control, Icarus, 174, 336–359, https://doi.org/10.1016/j.icarus.2004.07.030, 2005.

Marrero, S. M., Phillips, F. M., Borchers, B., Lifton, N., Aumer, R., and Balco, G.: Cosmogenic Nuclide Systematics and the CRONUScalc Program, Quat. Geochronol., 31, 160–187, https://doi.org/10.1016/j.quageo.2015.09.005, 2016.

Matsuoka, N.: Temporal and Spatial Variations in Periglacial Soil Movements on Alpine Crest Slopes, Earth Surf. Process. Landforms, 30, 41–58, https://doi.org/10.1002/esp.1125, 2005.

Messerli, B. and Winiger, M.: Climate, Environmental Change, and Resources of the African Mountains from the Mediterranean to the Equator, Mt. Res. Dev., 12, 315–336, https://doi.org/10.2307/3673683, 1992.

Miehe, S. and Miehe, G.: Ericaceous Forests and Heathlands in the Bale Mountains of South Ethiopia - Ecology and Man's Impact, Stiftung Walderhaltung in Afrika, Hamburg, 1994.

Miller, R., Common, R., and Galloway, R. W.: Stone Stripes and Other Surface Features of Tinto Hill, Geogr. J., 120, 216, https://doi.org/10.2307/1791537, 1954.

Mohr, P.: Ethiopian Flood Basalt Province, Nature, 303, 577–584, https://doi.org/10.1038/303577a0, 1983.

Mulheran, P. A.: Theory of Self-Organisation in Sorted Stone Stripes, J Phys, 4, 1–5, 1994.

Nicholson, F. H.: Patterned Ground Formation and Description as Suggested by Low Arctic and Subarctic Examples, Arctic and Alpine Research, 8, 329, https://doi.org/10.2307/1550437, 1976.

Osmaston, H. A., Mitchell, W. A., and Osmaston, J. A. N.: Quaternary Glaciation of the Bale Mountains, Ethiopia, J. Quat. Sci., 20, 593–606, https://doi.org/10.1002/jqs.931, 2005.

Ossendorf, G., Groos, A. R., Bromm, T., Tekelemariam, M. G., Glaser, B., Lesur, J., Schmidt, J., Akçar, N., Bekele, T., Beldados, A., Demissew, S., Kahsay, T. H., Nash, B. P., Nauss, T., Negash, A., Nemomissa, S., Veit, H., Vogelsang, R., Woldu, Z., Zech, W., Opgenoorth, L., and Miehe, G.: Middle Stone Age Foragers Resided in High Elevations of the Glaciated Bale Mountains, Ethiopia, Science, 365, 583–587, https://doi.org/10.1126/science.aaw8942, 2019.

Richmond, G. M.: Stone Nets, Stone Stripes, and Soil Stripes in the Wind River Mountains, Wyoming, Geol. J., pp. 143–153, 1949.

Seleshi, Y. and Zanke, U.: Recent Changes in Rainfall and Rainy Days in Ethiopia, Int. J. Climatol., 24, 973–983, https://doi.org/10.1002/joc.1052, 2004.

Steinemann, O., Reitner, J. M., Ivy-Ochs, S., Christl, M., and Synal, H.-A.: Tracking rockglacier evolution in the Eastern Alps from the Lateglacial to the early Holocene, Quat. Sci. Rev., 241, 1–19, https://doi.org/10.1016/j.quascirev.2020.106424, 2020.

Tierney, J. E., Russell, J. M., Huang, Y., Damsté, J. S. S., Hopmans, E. C., and Cohen, A. S.: Northern Hemisphere Controls on Tropical Southeast African Climate During the Past 60,000 Years, Science, 322, 252–255, https://doi.org/10.1038/nature02251, 2008.

Tierney, J. E., Russell, J. M., Sinninghe Damsté, J. S., Huang, Y., and Verschuren, D.: Late Quaternary Behavior of the East African Monsoon and the Importance of the Congo Air Boundary, Quat. Sci. Rev., 30, 798–807, https://doi.org/10.1016/j.quascirev.2011.01.017, 2011.

Umer, M., Kebede, S., and Osmaston, H. A.: Quaternary Glacial Activity on the Ethiopian Mountains, in: Developments in Quaternary Sciences, vol. 2 of *Quaternary Glaciations - Extent and Chronology, Part IIII*, pp. 171–174, Elsevier, Amsterdam, ehlers, j., gibbard, p. l. edn., https://doi.org/10.1016/S1571-0866(04)80122-2, 2004.

Vieira, G., Mora, C., and Faleh, A.: New Observations Indicate the Possible Presence of Permafrost in North Africa (Djebel Toubkal, High Atlas, Morocco), Cryosphere, 11, 1691–1705, https://doi.org/10.5194/tc-11-1691-2017, 2017.

Viste, E. and Sorteberg, A.: Moisture Transport into the Ethiopian Highlands, Int. J. Climatol., 33, 249–263, https://doi.org/10.1002/joc.3409, 2013.

Vockenhuber, C., Miltenberger, K.-U., and Synal, H.-A.: ^{36}Cl Measurements with a Gas-Filled Magnet at 6 MV, Nucl. Instrum. Methods Phys. Res. B, 455, 190–194, https://doi.org/10.1016/j.nimb.2018.12.046, 2019.

Vopata, J., Aber, J. S., and Kalm, V.: Patterned Ground in the Culebra Range, Southern Colorado, ESRS, 43, 8–21, 2006.

Washburn, A.: Permafrost Features as Evidence of Climatic Change, Earth-Sci. Rev., 15, 327–402, https://doi.org/10.1016/0012-8252(80)90114-2, 1980.

Werner, B. and Hallet, B.: Numerical Simulation of Self-Organized Stone Stripes, Nature, 361, 1993.

Wicky, J. and Hauck, C.: Air Convection in the Active Layer of Rock Glaciers, Front. Earth Sci., 8, 1–17, https://doi.org/10.3389/feart.2020.00335, 2020.

Williams, F.: Safeguarding Geoheritage in Ethiopia: Challenges Faced and the Role of Geotourism, Geoheritage, 12, 1–22, https://doi.org/10.1007/s12371-020-00436-9, 2020.

Wilson, P., Bentley, M. J., Schnabel, C., Clark, R., and Xu, S.: Stone Run (Block Stream) Formation in the Falkland Islands over Several Cold Stages, Deduced from Cosmogenic Isotope (^{10}Be and ^{26}Al) Surface Exposure Dating, J. Quat. Sci., 23, 461–473, https://doi.org/10.1002/jqs.1156, 2008.

Wöllauer, S., Zeuss, D., Hänsel, F., and Nauss, T.: TubeDB: An on-demand processing database system for climate station data, Computers & Geosciences, 146, 2–10, https://doi.org/10.1016/j.cageo.2020.104641, 2020.